ELSEVIER

Physica D 170 (2002) 206–252

PHYSICA D

www.elsevier.com/locate/physd

A priori tests of a stochastic mode reduction strategy

A. Majda [a,b], I. Timofeyev [a,b], E. Vanden-Eijnden [a,*]

[a] *Courant Institute of Mathematical Sciences, New York University, New York, NY 10012, USA*
[b] *Center for Atmosphere Ocean Science, New York University, New York, NY 10012, USA*

Received 26 November 2001; received in revised form 13 June 2002; accepted 24 June 2002
Communicated by C.K.R.T. Jones

Abstract

Several a priori tests of a systematic stochastic mode reduction procedure recently devised by the authors [Proc. Natl. Acad. Sci. 96 (1999) 14687; Commun. Pure Appl. Math. 54 (2001) 891] are developed here. In this procedure, reduced stochastic equations for a smaller collections of resolved variables are derived systematically for complex nonlinear systems with many degrees of freedom and a large collection of unresolved variables. While the above approach is mathematically rigorous in the limit when the ratio of correlation times between the resolved and the unresolved variables is arbitrary small, it is shown here on a systematic hierarchy of models that this ratio can be surprisingly big. Typically, the systematic reduced stochastic modeling yields quantitatively realistic dynamics for ratios as large as 1/2. The examples studied here vary from instructive stochastic triad models to prototype complex systems with many degrees of freedom utilizing the truncated Burgers–Hopf equations as a nonlinear heat bath. Systematic quantitative tests for the stochastic modeling procedure are developed here which involve the stationary distribution and the two-time correlations for the second and fourth moments including the resolved variables and the energy in the resolved variables. In an important illustrative example presented here, the nonlinear original system involves 102 degrees of freedom and the reduced stochastic model predicted by the theory for two resolved variables involves both nonlinear interaction and multiplicative noises. Even for large value of the correlation time ratio of the order of 1/2, the reduced stochastic model with two degrees of freedom captures the essentially nonlinear and non-Gaussian statistics of the original nonlinear systems with 102 modes extremely well. Furthermore, it is shown here that the standard regression fitting of the second-order correlations alone fails to reproduce the nonlinear stochastic dynamics in this example.

PACS: 02.50.−r; 02.70.Rw; 05.20.−y; 05.70.Ln

Keywords: Stochastic modeling; Mode reduction; Stationary distribution; Non-Gaussian statistics; Truncated Burgers–Hopf system

1. Introduction

Despite the rapid improvement of computer performance, many problems of scientific and engineering interest will not be amenable to direct numerical simulations in the foreseeable future. To list a few, the dynamics of the coupled atmosphere/ocean system [1], the folding of a large protein in macromolecular dynamics [2], or the epitaxial growth of a crystal in material science [3,4], each of these problems involves such a huge number of

* Corresponding author.
E-mail address: eve2@cims.nyu.edu (E. Vanden-Eijnden).

0167-2789/02/$ – see front matter
PII: S0167-2789(02)00578-X

degrees of freedom interacting on so many different space–time-scales that they vastly overwhelm direct numerical computations. On the other hand, while a complete description of the dynamics in these examples is impossible, it is also not necessarily useful since one is typically interested only in a few more essential degrees of freedom in the system which evolve slowly on the largest scales. In the above examples, these essential degrees of freedom might be a few large scale telleconnection patterns in the atmosphere, a few angles describing large conformational changes in the protein, or the position of a few steps edges on the crystal surface. There is therefore a real need for modeling strategies able to provide closed simplified equations for the dynamics of essential degrees of freedom alone by systematic elimination of all the other modes. Such a systematic mode elimination strategy was proposed and developed in detail by the authors in [5,6] (for different approaches to this question, see, e.g. [7–10]). The aim of the present work is to illustrate the method on a systematic family of non-trivial test cases which bear some of the features of the motivating examples listed above and to asses their performance in regimes with large values of the coupling parameters.

The mode elimination technique proposed in [5,6] is a two step procedure based on the assumption that the degrees of freedom in the system under consideration have been split into a set of essential modes we wish to describe and a set with all the other modes we wish to eliminate. The essential modes in the first set will be referred to as the resolved ones, and the unessential modes in the other set as the unresolved ones. In the first step of the procedure, the equations of motion for the unresolved modes are modified by representing the nonlinear self-interaction terms between unresolved modes by stochastic terms. The motivation is that the self-interaction terms are responsible for the sensitive dependence on small perturbations in the system on short time-scales and they can indeed be represented adequately by stochastic terms if coarse-grained modeling on longer time-scales is the objective. In the second step of the procedure, the equations of motion for the unresolved modes are then eliminated using standard projection techniques for stochastic differential equations [11–14]. The elimination step is rigorous in the limit where the stochastic terms are infinitely fast, corresponding to situations where the unresolved modes evolve much faster than the resolved ones.

This mode elimination technique has two obvious advantages. First, the ad hoc simplification of the original dynamics is made on the level of the equations for the unresolved modes and not the resolved ones. This is unlike most modeling strategies found in the literature where one starts with the equations for the resolved modes, drops all terms involving the unresolved modes in these equations, and replaces them by ad hoc stochastic terms, usually of linear Langevin-type, with parameters obtained by regression fit (see the bibliography of [6] for several examples). In contrast, our technique systematically gives the structure of the stochastic terms in the equations for the resolved modes, and it was shown in [5,6] that this structure is surprisingly rich: nonlinear correction arise, linear Langevin terms which can be both stabilizing or destabilizing, multiplicative noises, as well as the modification of such effects through dispersion. The second advantage of the technique is its rigor in some appropriate limiting parameter range which can be deduced a priori from the original equations. This provides a guideline for the applicability of the method, which is also an important new feature.

In this paper, we shall illustrate both advantages of the approach on some non-trivial test cases which demonstrate the feasibility and effectiveness of the method. At the same time, this will allow us to discuss some typical phenomena we may expect for more general systems; they are related to the special structure of the reduced equations for the resolved modes which is predicted.

In Section 2, we will first discuss simple triad systems. Triads have the generic nonlinear structure of any larger system involving quadratic nonlinear interactions, and we will show that they fit into two types. The first (studied in Section 2.1) will be referred to as the additive type and is such that the nonlinear interaction in the equation for the (single) resolved mode involve two unresolved modes. In this case the reduced equations are linear Langevin equations of Ornstein–Uhlenbeck type. The second type (studied in Section 2.2) will be refereed to as the multiplicative type and is such that the nonlinear interaction in the equations for the (two) resolved modes involve

one resolved and one unresolved modes. In this case the reduced equations contain nonlinear corrections in the resolved modes as well as multiplicative noises, and these unusual features are shown to be crucial to reproduce adequately the original dynamics. Beside discussing the phenomena in triad systems, we also show how to determine explicitly the regime of validity of the mode elimination technique even though there is no small parameter explicit in the original equations. The mode elimination technique turns out to be applicable on a surprisingly large range of parameters which is a potentially important practical feature.

In the triad examples, we start with stochastic differential equations. Hence, these examples are void for the stochastic modeling step in our technique. This step is illustrated and discussed in detail in Section 3 where we consider extensions of the truncated Burgers–Hopf system introduced in [15,16] by two of the authors. The truncated Burgers–Hopf system is a purely deterministic system which displays features common with vastly more complicated models such as the examples cited before and makes it an ideal test case for mode elimination technique. We use extensions of the truncated Burgers–Hopf system where the original degrees of freedom in these equations, taken as the unresolved ones, are coupled to one or two essential degrees of freedom. In these examples, the effectiveness of the stochastic modeling step in our technique can be assessed in detail and we show that we can achieve very good stochastic consistency between a suitable stochastic model and the original equations. A closed set of reduced equations for the resolved modes alone is then obtained by suitable projection following the general strategy in [5,6]. As in the triad system, we consider extensions of the truncated Burgers–Hopf system in an additive (Section 3.2) and a multiplicative (Section 3.3) settings. We also study an extension involving both types combined in Section 3.4. We discuss in detail the phenomena described by the reduced equation and show that their specific structure is essential to reproduce correctly non-trivial features of the original dynamics, including the stationary distribution and two-time statistical moments of order up to 4. In fact, if the reader were to pick a single example in the paper demonstrating the power of the methods developed in [5,6] as a preview, it should be the multiplicative one in Section 3.3. In this example, there is only a moderate separation of time-scale between resolved and unresolved modes. The stochastic model does an excellent job here, demonstrating almost complete stochastic consistency with the original system both at the level of the resolved and the unresolved modes, even regarding tests involving two-time fourth-order moments. The reduced equations obtained through mode elimination for only two resolved modes out of the 102 modes in the original system also do very well. For instance, these reduced equations reproduce the essentially nonlinear and non-Gaussian statistics of the original system extremely well. Furthermore, it is shown there that a linear Langevin-type model based on standard regression fitting of the second-order correlations fails to reproduce the nonlinear dynamics.

2. Elementary triad models

Triad systems where three modes interact through quadratic nonlinear interactions provide a nice simple test case for our mode elimination strategy. The nonlinear coupling in triad systems is generic of nonlinear coupling between any three modes in larger systems with quadratic nonlinearity [5,6]. In this section, we shall consider the two generic cases where: (i) one of the three modes is identified as the resolved variable and the other two as unresolved, and (ii) two of the modes are identified as resolved variables and the other one as unresolved. In case (i), which we shall refer to as the *additive case*, we will show that the reduced equation is a linear Langevin equation of Ornstein–Uhlenbeck type which, surprisingly enough, can be both stable or unstable depending on the parameters. In case (ii), which we shall refer to as the *multiplicative case*, the reduced equations involve both nonlinear correcting terms and multiplicative noises. In this case, the stationary distribution for the system (when it exists) is a quite complicated non-Gaussian distribution which will be exactly captured by the reduced equations.

In these examples we start from stochastic differential equations by adding appropriate forcing and damping terms in the equations for the unresolved variables. As a result, these examples do not address the issue of stochastic consistency but they clearly illustrate the main ideas behind the mode elimination theory as well as the role of the small parameter, ε. Here ε is not explicit in the original equations but is identified through careful non-dimensionalization. Numerical simulations show that the asymptotic theory is applicable and the solutions of the reduced equations and the original triad equations agree quantitatively up to $\varepsilon \approx 0.5$.

2.1. Additive triad model

The additive triad model consists of one resolved mode, v_1, and two unresolved modes, v_2 and v_3, satisfying

$$\frac{\mathrm{d}v_1}{\mathrm{d}t} = B_1 v_2 v_3, \qquad \frac{\mathrm{d}v_2}{\mathrm{d}t} = B_2 v_1 v_3 - \gamma_2 v_2 + \sigma_2 \dot{W}_2(t), \qquad \frac{\mathrm{d}v_3}{\mathrm{d}t} = B_3 v_1 v_2 - \gamma_3 v_3 + \sigma_3 \dot{W}_3(t). \tag{1}$$

We shall obtain a closed equation for v_1 alone by suitable elimination of v_2, v_3. As we will see, the reduced equation for v_1 is linear in v_1 with an additive noise, i.e. it determines an Ornstein–Uhlenbeck process.

2.1.1. Stationary distribution

In order to apply the mode elimination strategy to (1) we first establish the order of magnitude of the different terms in these equations. We do this by analyzing the stationary distribution for the dynamics in (1). By non-dimensionalization we will then determine ε in terms of the other parameters.

The Fokker–Planck operator associated with the Ornstein–Uhlenbeck part of the stochastic model (damping and white-noise forcing only) in (1) annihilates exactly the Gaussian density distribution

$$\bar{p}(v_2, v_3) = Z^{-1} \exp\left(-\frac{\gamma_2}{\sigma_2^2} v_2^2 - \frac{\gamma_3}{\sigma_3^2} v_3^2 \right), \tag{2}$$

where here and below Z is a constant of normalization whose value may change from line to line. On the other hand, the deterministic dynamics in (1) possess three Manley–Rowe relations as quadratic invariant:

$$M_{12} = B_1 v_2^2 - B_2 v_1^2, \qquad M_{13} = B_1 v_3^2 - B_3 v_1^2, \qquad M_{23} = B_2 v_3^2 - B_3 v_2^2. \tag{3}$$

Any two quantities amongst those in (3) are linearly independent and the other one can be obtained as linear combinations of these two. Under the additional assumption that the coupling constants B_1, B_2, B_3 satisfy

$$B_1 + B_2 + B_3 = 0, \tag{4}$$

the deterministic dynamics in (1) also conserves the energy

$$E = v_1^2 + v_2^2 + v_3^2, \tag{5}$$

which again can be expressed as a linear combination of two Manley–Rowe relations. Here, we consider the general case where (4) is not necessarily satisfied.

Since the Manley–Rowe relations are conserved by the deterministic dynamics, it follows that the Liouville operator associated with the quadratic nonlinear terms in (1) annihilates exactly any Gaussian distribution with a density of the type

$$p(v_1, v_2, v_3) = Z^{-1} \exp(-\beta_2 M_{12} - \beta_3 M_{13}). \tag{6}$$

Here β_1, β_3 are arbitrary constants and for convenience we picked M_{12}, and M_{13} as the two primary Manley–Rowe relations. In order that (6) be the unique stationary distribution for the full dynamics in (1) we must require the

following two properties: (i) (6) must be consistent with (2), and (ii) (6) must be normalizable. Requirement (i) is $\int_{\mathbf{R}} p\,\mathrm{d}v_1 = \bar{p}$, and it is satisfied if

$$\beta_2 = \frac{\gamma_2}{B_1\sigma_2^2}, \qquad \beta_3 = \frac{\gamma_3}{B_1\sigma_3^2}. \tag{7}$$

For requirement (ii), we use (7), and write (6) explicitly as

$$p(v_1, v_2, v_3) = Z^{-1} \exp\left(-\frac{v_1^2}{2C_1} - \frac{v_2^2}{2C_2} - \frac{v_3^2}{2C_3}\right), \tag{8}$$

where

$$C_1 = -\frac{\sigma_2^2\sigma_3^2 B_1}{2\gamma_2\gamma_3(B_2\gamma_2\sigma_3^2 + B_3\gamma_3\sigma_2^2)}, \qquad C_2 = \frac{\sigma_2^2}{2\gamma_2}, \qquad C_3 = \frac{\sigma_3^2}{2\gamma_3}. \tag{9}$$

(C_1 can also be written as $C_1 = -B_1C_2C_3/(B_2C_3 + B_3C_2)$.) The quantities C_1, C_2, and C_3 are the respective variances of the modes v_1, v_2, and v_3 computed with the measure associated with (8), and requirement (ii) is satisfied if and only if

$$C_1 > 0. \tag{10}$$

It is clear from (9) that (10) is not always satisfied. For $C_1 \leq 0$, (8) cannot be the stationary distribution for the dynamics in (1) and, in fact, our analysis suggests that there is no stationary distribution in this case (note that we can have $C_1 \leq 0$ even if (4) is satisfied, i.e. even if the deterministic dynamics in (1) conserves the energy (5)). The non-existence of a stationary distribution for the dynamics in (1) for suitable B_1, B_2, and B_3 means that in such regimes the backscatter of energy from mode v_1 to modes v_2 and v_3 where the dissipation occurs is insufficient, and the variance of mode v_1 then increases without bound. Both the existence of a stationary distribution with the Gaussian density in (8) if $C_1 > 0$ and the non-existence of a stationary distribution if $C_1 \leq 0$ were confirmed numerically. In Fig. 1 the Gaussian density for mode v_1 alone obtained by projection of (8) is compared to the density obtained from numerical simulations for a typical value of the parameters such that $C_1 > 0$. The agreement is excellent. (Note that in Fig. 1 and elsewhere in this paper, a logarithmic scale is utilized in plotting probability density functions.) Fig. 2 shows the unaveraged $v_1(t)$ for a typical value of the parameters such that $C_1 < 0$. As expected $v_1(t)$ grows unboundedly in time. Let us point out finally that the reduced equation for v_1 obtained below by mode elimination leads to the correct Gaussian density if $C_1 > 0$ and confirms the non-existence of a stationary distribution for $C_1 \leq 0$.

2.1.2. Non-dimensionalization and determination of ε

Unless explicitly stated otherwise from now on we focus on the situation where stationary distribution exists, i.e. $C_1 > 0$. We also focus on the statistical equilibrium solution of the equations in (1) where the memory of the initial conditions is lost. We shall non-dimensionalize the equations in (1) in such a way that the small parameter ε necessary for the mode elimination procedure enters the equations and is explicitly determined in terms of the other parameters. We proceed in two steps. First we normalize the modes v_j by the square-root of their variance, i.e. we substitute

$$v_j \to \sqrt{C_j}v_j, \quad j = 1, 2, 3. \tag{11}$$

In terms of the new variables the equations in (1) become

$$\frac{\mathrm{d}v_1}{\mathrm{d}t} = b_1v_2v_3, \qquad \frac{\mathrm{d}v_2}{\mathrm{d}t} = b_2v_1v_3 - \gamma_2v_2 + \sqrt{2\gamma_2}\dot{W}_2(t), \qquad \frac{\mathrm{d}v_3}{\mathrm{d}t} = b_3v_1v_2 - \gamma_3v_3 + \sqrt{2\gamma_3}\dot{W}_3(t), \tag{12}$$

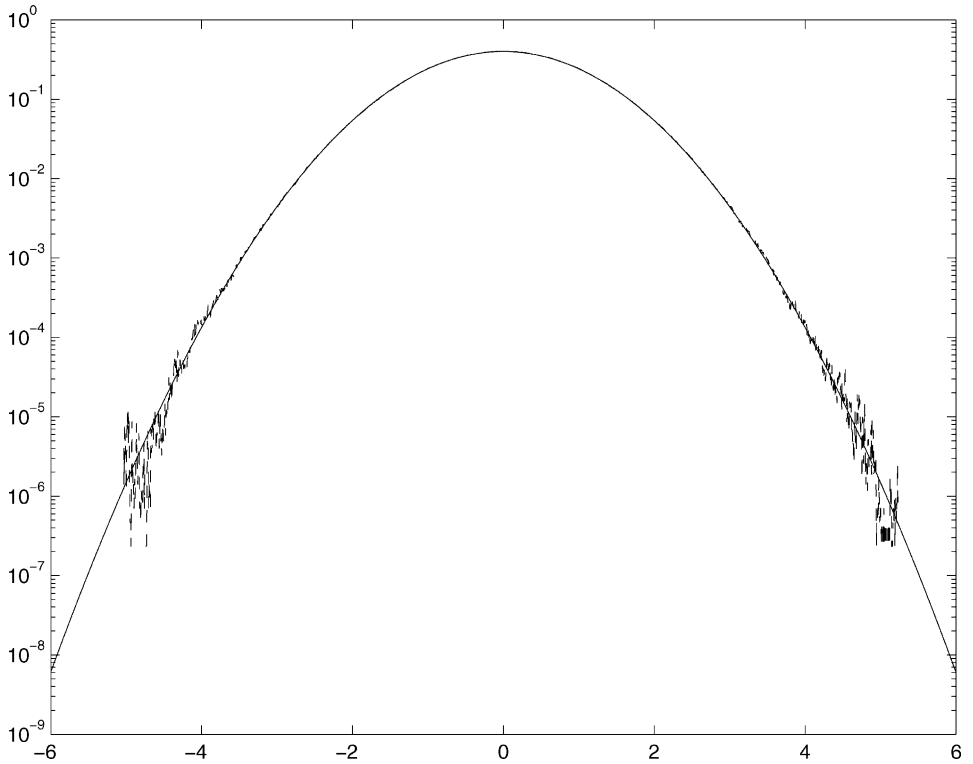

Fig. 1. Additive triad system. The Gaussian density in (8) compared with the density obtained from numerical simulations for $C_1 > 0$.

where

$$b_1 = B_1\frac{\sqrt{C_2C_3}}{\sqrt{C_1}}, \qquad b_2 = B_2\frac{\sqrt{C_1C_3}}{\sqrt{C_2}}, \qquad b_3 = B_3\frac{\sqrt{C_1C_2}}{\sqrt{C_3}}. \tag{13}$$

It can be checked by direct verification that

$$b_1 + b_2 + b_3 = 0. \tag{14}$$

By construction all the dependent variables v_j in (12) are in average of order 1. To proceed further we now renormalize time in such a way that the nonlinear terms in (12) are of order 1, i.e. we substitute (using (14) to represent $b_1 = -b_2 - b_3$)

$$t \to \frac{t}{b}, \quad b = \max(|b_2 + b_3|, |b_2|, |b_3|). \tag{15}$$

Using the new time variable (15) and assuming without loss of generality that $\gamma_2 \geq \gamma_3$ (for $\gamma_2 < \gamma_3$ relabel modes v_2, v_3), (12) becomes

$$\frac{\mathrm{d}v_1}{\mathrm{d}t} = \bar{b}_1 v_2 v_3, \qquad \frac{\mathrm{d}v_2}{\mathrm{d}t} = \bar{b}_2 v_1 v_3 - \frac{1}{\varepsilon\delta}v_2 + \sqrt{\frac{2}{\varepsilon\delta}}\dot{W}_2(t), \qquad \frac{\mathrm{d}v_3}{\mathrm{d}t} = \bar{b}_3 v_1 v_2 - \frac{1}{\varepsilon}v_3 + \sqrt{\frac{2}{\varepsilon}}\dot{W}_3(t), \tag{16}$$

where we define

$$\bar{b}_j = \frac{b_j}{b}, \quad j = 1, 2, 3, \qquad \delta = \frac{\gamma_3}{\gamma_2} \in (0, 1], \qquad \varepsilon = \frac{b}{\gamma_3}. \tag{17}$$

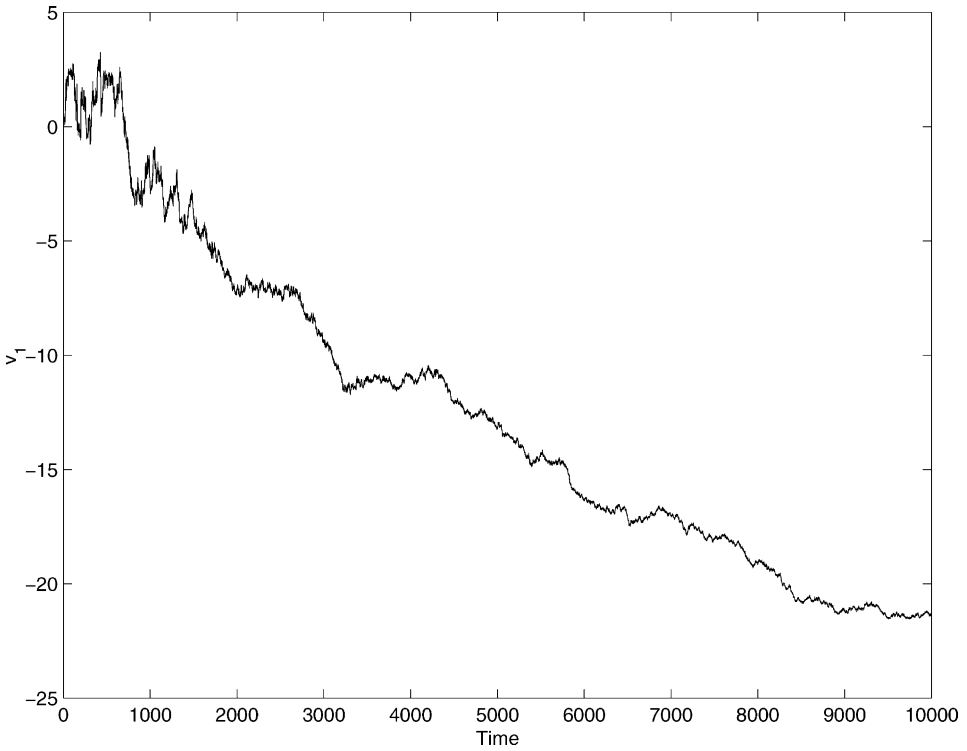

Fig. 2. Additive triad system. The unaveraged process $v_1(t)$ for a situation with $C_1 < 0$ where there is no stationary distribution: the process grows unboundedly in time.

Since all terms but the damping and forcing terms in (16) are on the average of order 1, ε as defined above is the correct parameter which need to be small for mode elimination. The role of ε in terms of time-scales of the modes v_1, v_2, and v_3 will be explained in the next section. More explicitly, ε is

$$\varepsilon = \gamma_3^{-1} \max\left(|B_1| \frac{\sqrt{C_2 C_3}}{\sqrt{C_1}}, |B_2| \frac{\sqrt{C_1 C_3}}{\sqrt{C_1}}, |B_3| \frac{\sqrt{C_1 C_2}}{\sqrt{C_3}} \right), \tag{18}$$

where the C_j's are given by (9).

In the remainder of this section, we may work with the dimensionless equations in (16) unless explicitly stated otherwise. At statistical equilibrium the solutions of (16) define a three-parameter family, $(\bar{b}_2, \bar{b}_3, \delta, \varepsilon)$, with either $\bar{b}_2$ or $\bar{b}_3$ or $\bar{b}_2 + \bar{b}_3$ equal to ± 1 by construction, the other two taking values in $[-1, 1]$, $\delta \in (0, 1]$, and $\varepsilon > 0$ arbitrary. Notice that the stationary distribution for (16) is a product of standard Gaussians with zero mean and unit variance. (Recall that (16) make sense only if a stationary distribution for the original equations in (1) exists, i.e. if (10) is satisfied, since otherwise we cannot change variables as in (11).) Of course, the two-time statistics of the process defined by (16) is still undetermined; next we study it by mode elimination.

2.1.3. Mode elimination

The detailed calculations for mode elimination in general systems with quadratic nonlinearity have been presented elsewhere [6]. The method is rigorously justified if ε in (18) is much smaller than 1. The range $\varepsilon \ll 1$ actually corresponds to situations where the maximum between the time-scales of the modes v_2 and v_3 is much smaller than

the time-scale of v_1. This can be checked upon noting that to leading order in $\varepsilon \ll 1$, (16) gives at statistical steady state

$$\langle v_2(t+s)v_2(s)\rangle = \mathrm{e}^{-|t|/\varepsilon\delta}, \qquad \langle v_3(t+s)v_3(s)\rangle = \mathrm{e}^{-|t|/\varepsilon}, \tag{19}$$

whereas the time-correlation function for v_1 will decay on a time-scale of the order of ε^{-1} (see (24)). Here we will see if the predictions of the theory can be utilized for large values of ε like $\varepsilon = 0.5$.

To leading order in ε, the mode elimination procedure (see [6]) gives the following equation for v_1 alone:

$$\frac{\mathrm{d}v_1}{\mathrm{d}t} = -\varepsilon\gamma v_1 + \sqrt{2\varepsilon}\sigma\dot{W}(t), \tag{20}$$

where

$$\gamma = \sigma^2 = \frac{(\bar{b}_2 + \bar{b}_3)^2}{1+\delta^{-1}}. \tag{21}$$

Note that coarse-graining time as $t \to t/\varepsilon$ as in [6] amounts to setting $\varepsilon = 1$ in (20). In fact, the theorem used to obtain (20) states that the solution of this equation converges to solution of the first equation in (16) for v_1 in the limit as $\varepsilon \to 0$ on the coarse-grained time-scale t/ε.

It is also interesting to consider (20) in the original variables

$$\frac{\mathrm{d}v_1}{\mathrm{d}t} = -\gamma' v_1 + \sigma'\dot{W}(t), \tag{22}$$

where

$$\gamma' = -\frac{B_1}{(\gamma_2+\gamma_3)}\left(\frac{B_3\sigma_2^2}{\gamma_2} + \frac{B_2\sigma_3^2}{\gamma_3}\right), \qquad \sigma' = \frac{\sigma_2\sigma_3|B_1|}{\sqrt{2\gamma_2\gamma_3(\gamma_2+\gamma_3)}}. \tag{23}$$

The Ornstein–Uhlenbeck process defined by (22) has a statistical steady state if and only if $\gamma' > 0$, which is equivalent to the constraint in (10). If this criterion is satisfied, the stationary distribution for the process in (22) is consistent with (8), and it reduces to the standard Gaussian for the non-dimensionalized process defined by (20) since $\sigma^2/\gamma = 1$ from (21). For $\gamma' < 0$, the unresolved modes v_2, v_3 actually pump energy in v_1. In fact, in the unstable case, the estimate in (18) is valid provided that one replaces the variances C_j computed on the stationary distribution by the instantaneous variances of the modes. Of course, in this case, ε becomes time dependent as well and it can be checked from (18) that ε grows as the variance of $v_1(t)$ grows. If the ε computed by replacing the C_j by the initial conditions $v_j^2(0)$ is small, the solution of (22) is a good approximation of the actual v_1 solution of (1) locally in time, but (22) eventually fails when ε becomes greater than 1.

2.1.4. Numerical simulations

We now compare the time-correlation function for the slow mode v_1 predicted from (20),

$$\langle v_1(t+s)v_1(s)\rangle = \mathrm{e}^{-\varepsilon\gamma|t|} \tag{24}$$

with the results of numerical integrations of the non-dimensional form of the triad equations in (16). We perform the simulations with

$$\bar{b}_1 = -0.75, \qquad \bar{b}_2 = -0.25, \qquad \bar{b}_3 = 1, \qquad \delta = 0.75 \tag{25}$$

for which the constraint in (10) for existence of the stationary distribution is satisfied and $\gamma = 0.24107$, and consider four values of ε

$$\varepsilon = 0.125, 0.25, 0.5, 1. \tag{26}$$

To integrate the triad equations in (16) we use time-splitting and utilize a second-order Runge–Kutta algorithm for the nonlinear coupling terms and the "exact solution" formula for the damping and forcing terms. The exact solution formula is the discrete analog of the integral representation of the exact solution of the Ornstein–Uhlenbeck process

$$\frac{\mathrm{d}x}{\mathrm{d}t} = -\gamma x + \sigma \dot{W}(t),$$

and is given by

$$x(t + \Delta t) = \mathrm{e}^{-\gamma \Delta t} x(t) + \sigma \eta_{\Delta t}(t),$$

where the $\eta_{\Delta t}(t)$'s are independent Gaussian random variables with mean zero and variance

$$\langle \eta^2_{\Delta t}(t) \rangle = \frac{1 - \mathrm{e}^{-2\gamma \Delta t}}{2\gamma}.$$

Finally, the statistics here and elsewhere are computed using time-averaging since the underlying stochastic model is ergodic.

The time-correlation function for the slow mode, v_1, is presented in Fig. 3 together with analytical prediction in (24). The same is presented in Fig. 4 in logarithmic scale. The agreement is excellent for $\varepsilon = 0.125, 0.25, 0.5$, though (24) decays always faster than the actual time-correlation function for v_1. For $\varepsilon = 1$, though the time-correlation function for v_1 remains exponential, the discrepancy in correlation time is more than 30%. This is of course natural since we cannot expect the asymptotic procedure to work for all values of ε.

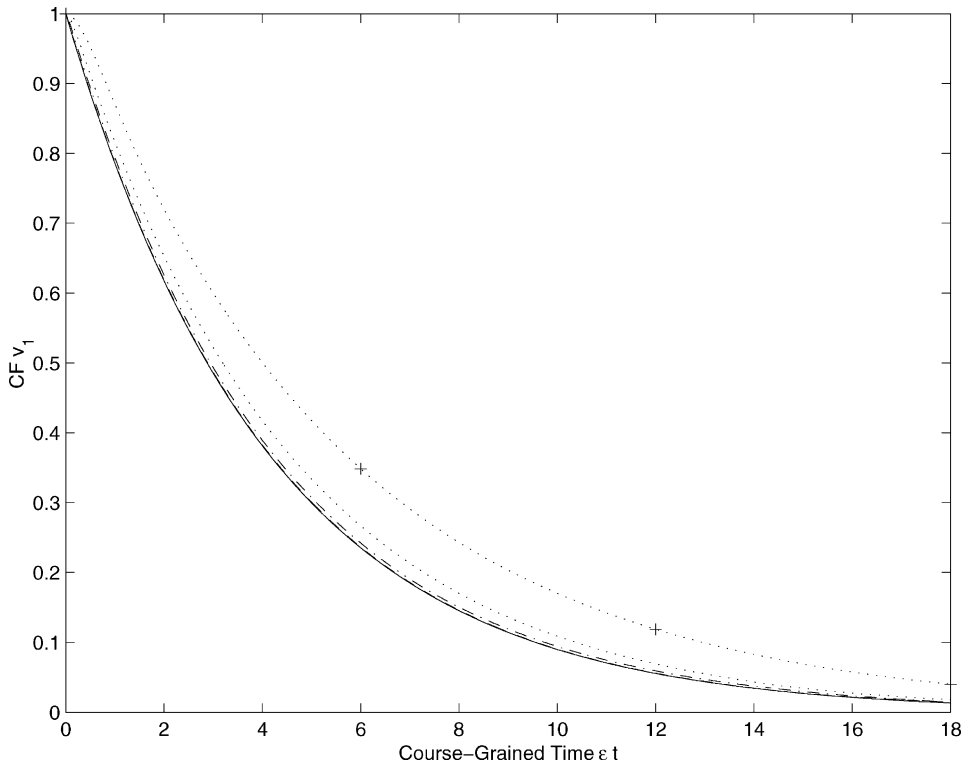

Fig. 3. Additive triad system. Time-correlation function of the resolved mode v_1. Solid line: prediction from mode elimination (20); dashed line: $\varepsilon = 0.125$; dot-dashed line: $\varepsilon = 0.25$; dotted line: $\varepsilon = 0.5$; dotted-plus line: $\varepsilon = 1$.

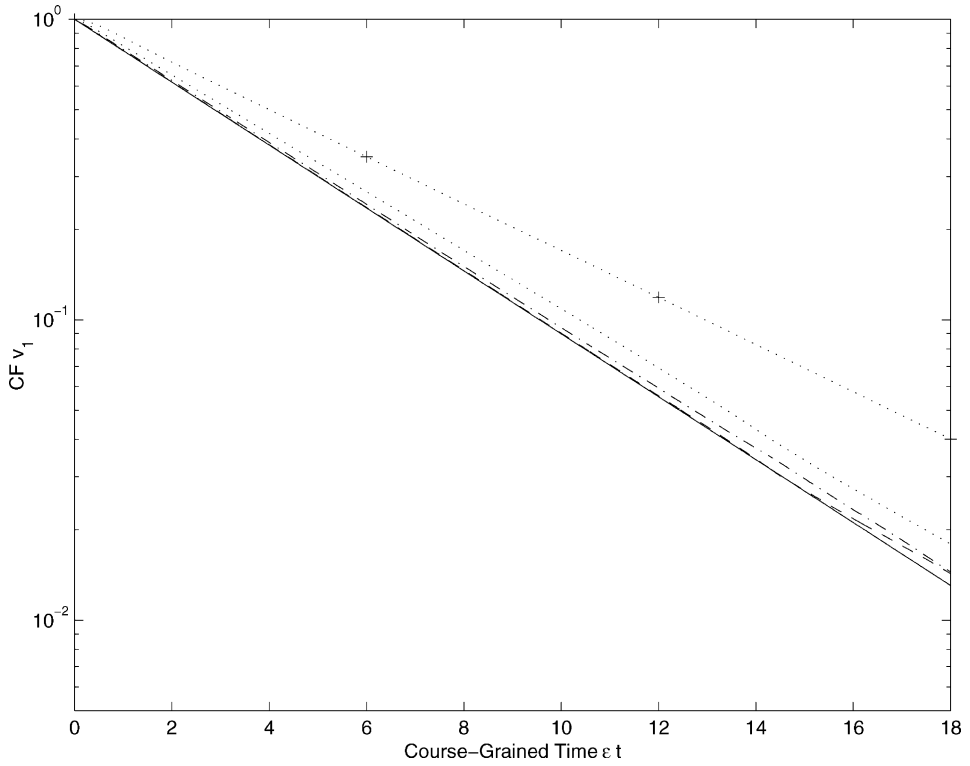

Fig. 4. Additive triad system. Same as in Fig. 3 in logarithmic scale.

We also tested higher order statistics of the mode v_1 using the following two-time four-order moment:

$$K_1(t) = \frac{\langle v_1^2(t+s)v_1^2(s)\rangle}{\langle v_1^2\rangle^2 + 2\langle v_1(t+s)v_1(s)\rangle^2}. \tag{27}$$

This statistical quantity is very natural since it measures how much the "energy" $v_1^2(t)$ correlates with itself at later time. The reduced equation in (20) predicts that the process is Gaussian, which implies that $K_1(t) = 1$ for all time. The quantity $K_1(t)$ is plotted in Fig. 5 for four values of ε. For $\varepsilon = 0.125, 0.25$ the process is fairly Gaussian, but as the value of ε increased we observe departure from Gaussianity not captured by (20). At the large value of $\varepsilon = 0.5$ the peak departure is still below 10%, but it exceeds 20% for $\varepsilon = 1$. It should be pointed out that later on in Section 2.2 about multiplicative triad systems (and then again in Sections 3.3 and 3.4 for systems with many degrees of freedom) we will observe systematic departure from Gaussianity even at small ε which are correctly captured by the reduced equations. In fact, Fig. 5 should be compared with Fig. 12 (the vertical scales are identical on these two figures).

2.2. Multiplicative triad model

The multiplicative triad model consists of two resolved modes, v_1 and v_2, and one unresolved mode, v_3, satisfying (compare (1))

$$\frac{\mathrm{d}v_1}{\mathrm{d}t} = B_1 v_2 v_3, \qquad \frac{\mathrm{d}v_2}{\mathrm{d}t} = B_2 v_1 v_3, \qquad \frac{\mathrm{d}v_3}{\mathrm{d}t} = B_3 v_1 v_2 - \gamma_3 v_3 + \sigma_3 \dot{W}_3(t). \tag{28}$$

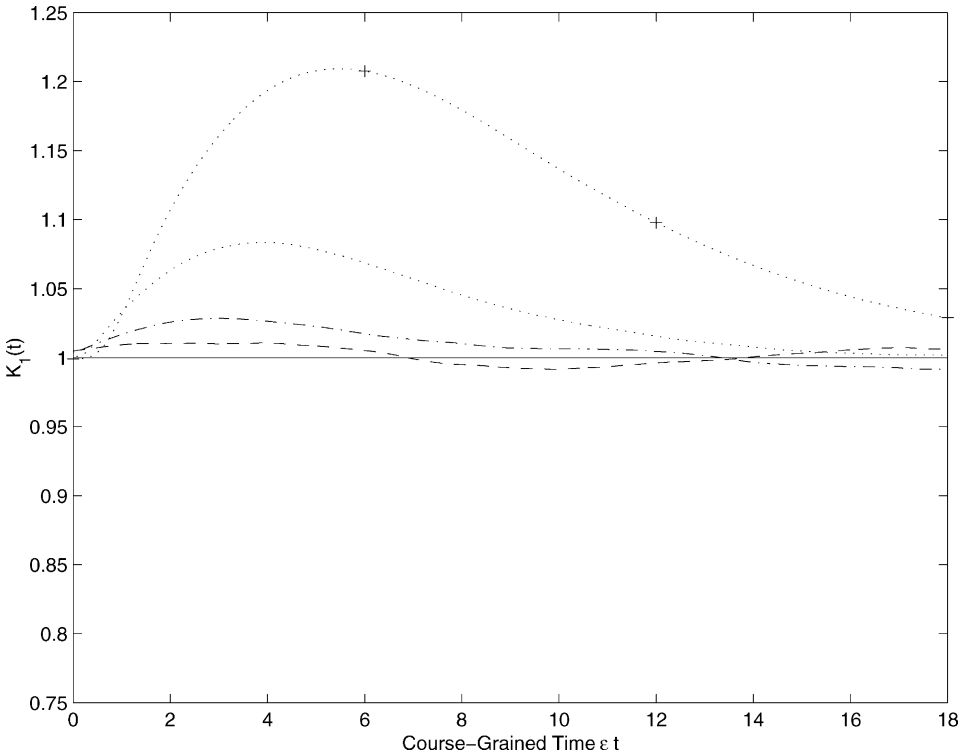

Fig. 5. Additive triad system. The two-time fourth-order moment $K_1(t)$ defined in (27). Dashed line: $\varepsilon = 0.125$; dot-dashed line: $\varepsilon = 0.25$; dotted line: $\varepsilon = 0.5$; dotted-plus line: $\varepsilon = 1$. The reduced equation in (20) predicts a Gaussian $v_1(t)$ for which $K_1(t) = 1$.

A closed set of equations for v_1 and v_2 alone will be obtained by elimination of v_3 in the appropriate limit. Since the right-hand sides of the equations for v_1 and v_2 in (28) contain the products v_1v_3 and v_2v_3, we can expect that the equation for v_1 and v_2 obtained by mode elimination will contain nonlinear corrections as well as multiplicative noises. Below, we confirm this intuition.

2.2.1. *Stationary distribution*

We proceed as in the additive case and first evaluate the order of magnitude of the different terms in (28) on the stationary distribution associated with these equations. This will again allow for non-dimensionalization of the equations and will give us ε in terms of the other parameters.

The important difference with the additive case which will actually lead to interesting new phenomena is that the Manley–Rowe relation

$$M_{12} = B_1 v_2^2 - B_2 v_1^2, \tag{29}$$

is conserved by the full dynamics (i.e. with damping and forcing on v_3 included) in (28). Denote by M_{12}^0 the initial value of M_{12}. Conservation of (29) implies that v_1 and v_2 move either on the ellipse $B_1 v_2^2 - B_2 v_1^2 = M_{12}^0$ if $B_1 B_2 < 0$, or on the hyperbola $B_1 v_2^2 - B_2 v_1^2 = M_{12}^0$ if $B_1 B_2 > 0$. In the latter case the motion is also restricted on one branch of the hyperbola, since the sign of v_1 is conserved if $B_1 M_{12}^0 > 0$, while the sign of v_2 is conserved if $B_1 M_{12}^0 < 0$. Combining all this we deduce that the following density is conserved by the Liouville operator

associated with the quadratic nonlinear terms in (28):

$$p(v_1, v_2, v_3) = Z^{-1} \exp(-\beta M_{13}) \delta(M_{12} - M_{12}^0) G(v_1, v_2), \tag{30}$$

where

$$G(v_1, v_2) = ((B_1 B_2)_- + (B_1 B_2)_+ ((B_1 M_{12}^0)_+ H(v_1 v_1^0) + (B_1 M_{12}^0)_- H(v_2 v_2^0))). \tag{31}$$

Here $v_1^0 = v_1(0)$ and $v_2^0 = v_2(0)$ are the initial conditions for the first two equations in (28), β is an arbitrary constant, $\delta(\cdot)$ the Dirac distribution, $H(\cdot)$ the Heaviside distribution, $(z)_+ = \max(z, 0)$, $(z)_- = \min(z, 0)$, and we picked M_{13} as the additional primary Manley–Rowe relation besides M_{12} for (32). In (32), the Dirac distribution concentrates the measure on the set where the Manley–Rowe relation in (29) has fixed value. The function G is unity if this set (projected on any plane $v_3 = \text{cst}$) is an ellipse, and simply picks the correct branch if this set is a hyperbola. The density in (30) is explicitly

$$p(v_1, v_2, v_3) = Z^{-1} \exp(-\beta(B_1 v_3^2 - B_3 v_1^2)) \delta(B_1 v_2^2 - B_2 v_1^2 - M_{12}^0) G(v_1, v_2), \tag{32}$$

and it will be the stationary distribution for the dynamics in (28) if: (i) it can be made consistent for some β with the Gaussian density annihilated by the Fokker–Planck operator associated with the Ornstein–Uhlenbeck part of the dynamics for v_3

$$\bar{p}(v_3) = Z^{-1} \exp\left(-\frac{\gamma_3}{\sigma_3^2} v_3^2\right), \tag{33}$$

and (ii) it is normalizable. Consistency is achieved by taking

$$\beta = \frac{\gamma_3}{B_1 \sigma_3^2}, \tag{34}$$

which leads to

$$p(v_1, v_2, v_3) = Z^{-1} \exp\left(-\frac{\gamma_3}{\sigma_3^2} v_3^2 + \frac{\gamma_3}{\sigma_3^2} \frac{B_3}{B_1} v_1^2\right) \delta(B_1 v_2^2 - B_2 v_1^2 - M_{12}^0) G(v_1, v_2). \tag{35}$$

Note that the factor $\gamma_3 B_3 v_1^2 / \sigma_3^2 B_1$ can also be written as $\gamma_3 B_3 v_2^2 / \sigma_3^2 B_2$ using the Dirac distribution, which shows that (35) is symmetric in the indices 1 and 2 as it should be. Concerning normalizability of (35), if the Dirac distribution picks an ellipse in the space (v_1, v_2), i.e. if $B_1 B_2 < 0$, then (35) is obviously normalizable since it is concentrated on a finite curve in any plane $v_3 = \text{cst}$. On the other hand, if the Dirac distribution picks a hyperbola in the space (v_1, v_2), i.e. if $B_1 B_2 > 0$, then normalizability requires that the coefficient in front of v_1^2 in the exponential in (35) is negative, i.e. we must have $B_1 B_3 < 0$. On the other hand, if $B_1 B_2 > 0$ and $B_1 B_3 > 0$ (i.e. all three B_j have the same sign), (35) is not normalizable and our analysis suggests that there is no stationary distribution in this case. This was confirmed numerically (see Fig. 10). It is interesting to note that this cannot happen if the energy in (5) is conserved since the constraint in (4) then precludes that all the B_j's have the same sign. Thus, a stationary distribution always exists if the energy is conserved.

Unlike in the additive case, the stationary distribution associated with (28) is not unique. Indeed, the Manley–Rowe relation (29) (as well as the sign of v_1^0 or v_2^0) is information about the initial conditions which is never lost and picks exactly one amongst a family of possible stationary distributions with densities in (35) for the process defined by (28).

We checked the density in (35) by computing numerically the reduced densities for modes v_1 and v_2 and comparing these results with the actual reduced densities obtained by integration of (35)

$$p(v_1) = Z^{-1} \exp\left(\frac{\gamma_3}{\sigma_3^2}\frac{B_3}{B_1}v_1^2\right)\frac{H(B_1B_2v_1^2 + B_1M_{12}^0)}{\sqrt{B_1B_2v_1^2 + B_1M_{12}^0}}G_1(v_1),$$
$$p(v_2) = Z^{-1} \exp\left(\frac{\gamma_3}{\sigma_3^2}\frac{B_3}{B_2}v_2^2\right)\frac{H(B_1B_2v_2^2 - B_2M_{12}^0)}{\sqrt{B_1B_2v_2^2 - B_2M_{12}^0}}G_2(v_2), \tag{36}$$

where

$$G_1(v_1) = (B_1B_2)_- + (B_1B_2)_+((B_1M_{12}^0)_- + (B_1M_{12}^0)_+H(v_1v_1^0)),$$
$$G_2(v_2) = (B_1B_2)_- + (B_1B_2)_+((B_1M_{12}^0)_+ + (B_1M_{12}^0)_-H(v_2v_2^0)). \tag{37}$$

As can be seen in Figs. 6 and 7 for a typical situation where $B_1B_2 < 0$ (motion restricted to an ellipse) and in Figs. 8 and 9 for a typical situation where $B_1B_2 > 0$ (motion restricted to a hyperbola), the numerical results are in excellent agreement with the theoretical predictions in (36). Finally, Fig. 10 shows the unaveraged $v_1(t)$ and $v_2(t)$ for a typical situation where the stationary distribution does not exist: as expected, they grow unbounded in time.

Reproducing the density in (35) (projected on the space (v_1, v_2), which amounts to setting $v_3 = 0$ in (35)) with the closed set of equations for v_1 and v_2 obtained by mode elimination is a severe test for any such mode elimination

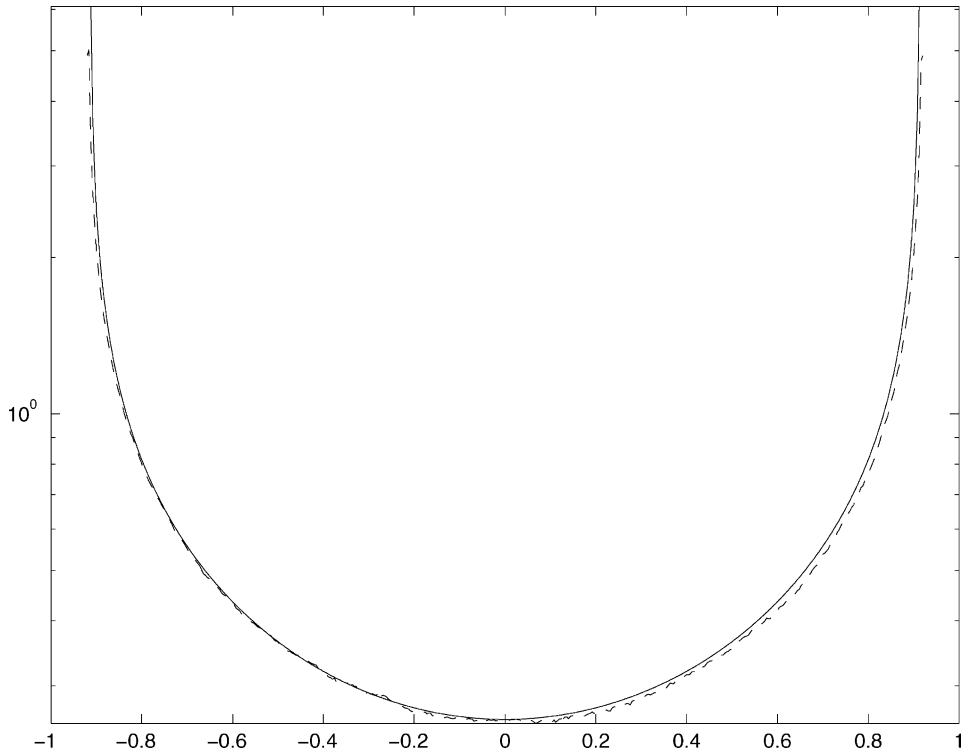

Fig. 6. Multiplicative triad system. Probability density for v_1 in (36) compared with the density obtained from numerical simulations for $B_1B_2 < 0$ (motion on an ellipse).

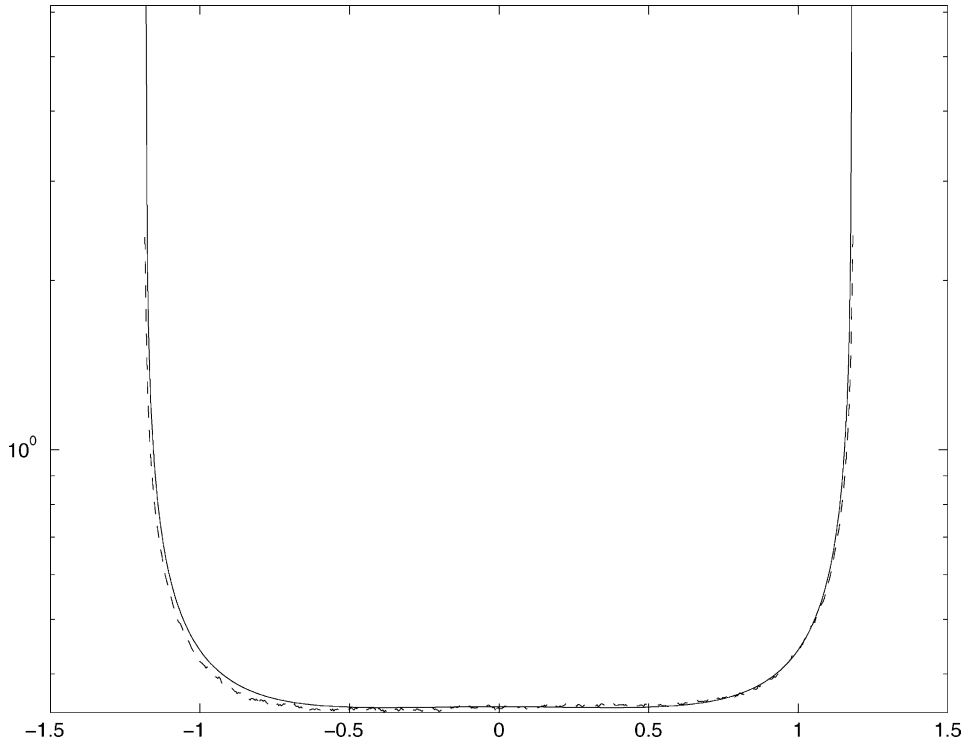

Fig. 7. Multiplicative triad system. Probability density for v_2 in (36) compared with the density obtained from numerical simulations for $B_1 B_2 < 0$ (motion on an ellipse).

procedure. We shall show below that the stationary distribution for the reduced equations for v_1 and v_2 which we obtain rigorously by the systematic procedure in [6] has a density given exactly by (35) (projected on the space (v_1, v_2)).

2.2.2. Non-dimensionalization and determination of ε

We now non-dimensionalize the equations in (28) and determine explicitly ε in terms of the other parameters. Throughout this section we assume that a stationary distribution for (28) exists, i.e. (35) is normalizable. We could proceed as in the additive case and normalize all the modes according to their root mean square computed from

$$C_j = \int_{\mathbf{R}^3} v_j^2 p(v_1, v_2, v_3)\, \mathrm{d}v_1\, \mathrm{d}v_2\, \mathrm{d}v_3, \quad j = 1, 2, 3. \tag{38}$$

The problem with this procedure is that, though convenient numerically, it leads to unpleasant analytical formulae because the second moments of the densities in (36) have rather involved expressions. For simplicity, we shall slightly modify the procedure in such a way that the parameter ε appearing in the non-dimensional equations obtained below is always an upper bound for the actual ε which would be obtained by normalizing the modes by their exact root mean squares (the actual ε is in fact given by (18) with the C_j's computed from (38)). For mode v_3, we simply use its variance, i.e. we substitute

$$v_3 \to \sqrt{C_3} v_3, \quad C_3 = \frac{\sigma_3^2}{2\gamma_3}. \tag{39}$$

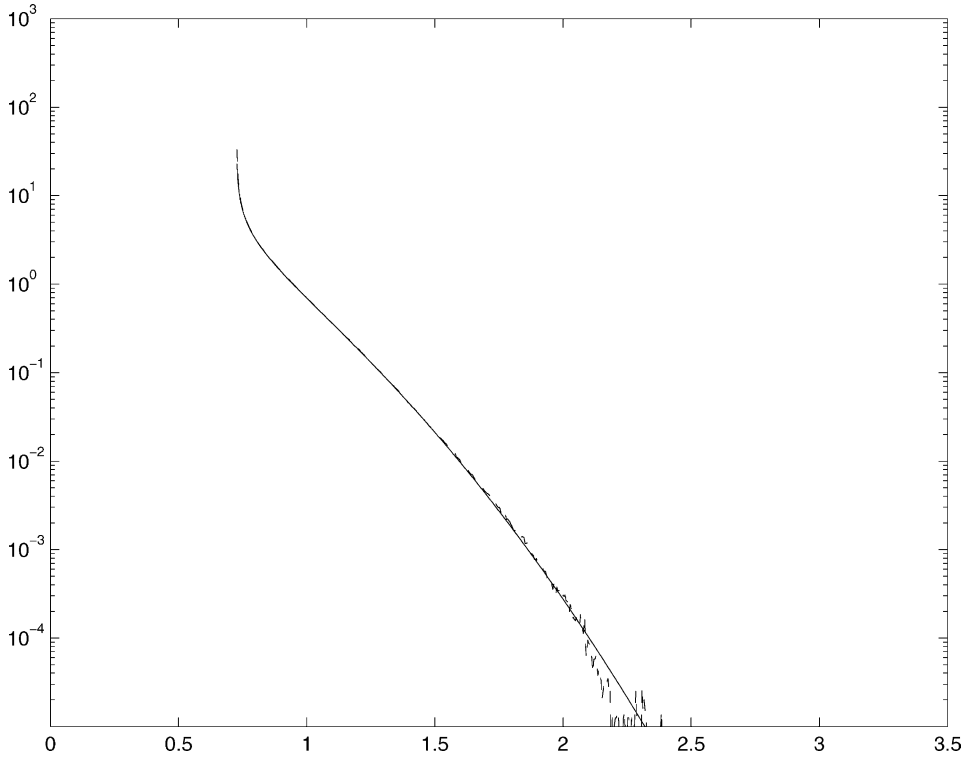

Fig. 8. Multiplicative triad system. Probability density for v_1 in (36) compared with the density obtained from numerical simulations for $B_1B_2 > 0$ (motion on one branch of a hyperbola).

For modes v_1, v_2, we always substitute

$$v_1 \to \sqrt{C_1}v_1, \qquad v_2 \to \sqrt{C_2}v_2, \tag{40}$$

but we use different C_1, C_2 if the motion is restricted to an ellipse or to a hyperbola. In the case of an ellipse, i.e. if $B_1B_2 < 0$, we simply take the tips of the ellipse as normalizing factors, i.e. we use

$$C_1 = \frac{|M_{12}^0|}{|B_2|}, \qquad C_2 = \frac{|M_{12}^0|}{|B_1|} \quad \text{if} \quad B_1B_2 < 0. \tag{41}$$

The exponential factors in (36) might actually restrict $v_1(t)$, $v_2(t)$ to some portion of the ellipse, but obviously C_1 and C_2 bound $v_1^2(t)$ and $v_2^2(t)$ for all times. In the case of a hyperbola, i.e. if $B_1B_2 > 0$, we use the variance computed from the Gaussian densities in (36) alone, but we add the square value of the tip of the hyperbola for the mode whose motion is restricted to the right or left of that tip. Thus, we use

$$C_1 = \frac{|B_3|\sigma_3^2}{2|B_1|\gamma_3} + \frac{|M_{12}^0|}{|B_2|}, \qquad C_2 = \frac{|B_3|\sigma_3^2}{2|B_2|\gamma_3} \quad \text{if} \quad B_1B_2 > 0 \ \text{ and } \ B_1M_{12}^0 < 0, \tag{42}$$

or

$$C_1 = \frac{|B_3|\sigma_3^2}{2|B_1|\gamma_3}, \qquad C_2 = \frac{|B_3|\sigma_3^2}{2|B_2|\gamma_3} + \frac{|M_{12}^0|}{|B_1|} \quad \text{if} \quad B_1B_2 > 0 \ \text{ and } \ B_1M_{12}^0 > 0. \tag{43}$$

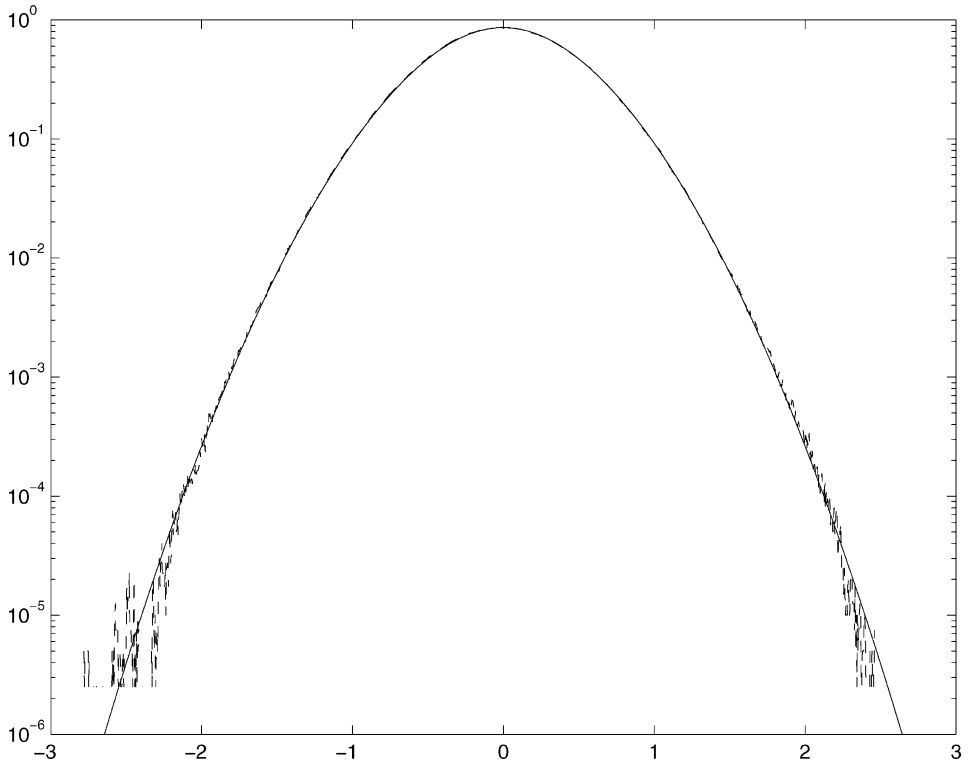

Fig. 9. Multiplicative triad system. Probability density for v_2 in (36) compared with the density obtained from numerical simulations for $B_1 B_2 > 0$ (motion on one branch of a hyperbola).

Again, on the average these C_1, C_2 overestimate the dynamical values for $v_1^2(t)$, $v_2^2(t)$. In terms of the new variables, the system in (28) becomes

$$\frac{\mathrm{d}v_1}{\mathrm{d}t} = b_1 v_2 v_3, \qquad \frac{\mathrm{d}v_2}{\mathrm{d}t} = b_2 v_1 v_3, \qquad \frac{\mathrm{d}v_3}{\mathrm{d}t} = b_3 v_1 v_2 - \gamma_3 v_3 + \sqrt{2\gamma_3}\dot{W}_3(t), \tag{44}$$

where the b_j's are defined as in (13) with the C_j's given above (meaning that they do not satisfy (14) in general). By construction all the dependent variables v_j in (44) are of order 1 or smaller. Next, we renormalize time as in (15), i.e. we substitute

$$t \to \frac{t}{b}, \quad b = \max(|b_1|, |b_2|, |b_3|). \tag{45}$$

The system in (44) then becomes

$$\frac{\mathrm{d}v_1}{\mathrm{d}t} = \bar{b}_1 v_2 v_3, \qquad \frac{\mathrm{d}v_2}{\mathrm{d}t} = \bar{b}_2 v_1 v_3, \qquad \frac{\mathrm{d}v_3}{\mathrm{d}t} = \bar{b}_3 v_1 v_2 - \frac{1}{\varepsilon} v_3 + \sqrt{\frac{2}{\varepsilon}}\dot{W}_3(t), \tag{46}$$

where we define

$$\bar{b}_j = \frac{b_j}{b}, \quad j = 1, 2, 3, \qquad \varepsilon = \frac{b}{\gamma_3}. \tag{47}$$

Since the three linear terms in (46) are of order 1 or smaller, we can conclude that the parameter ε entering (46) is an upper bound for the parameter which must be small for mode elimination. A more explicit expression for ε

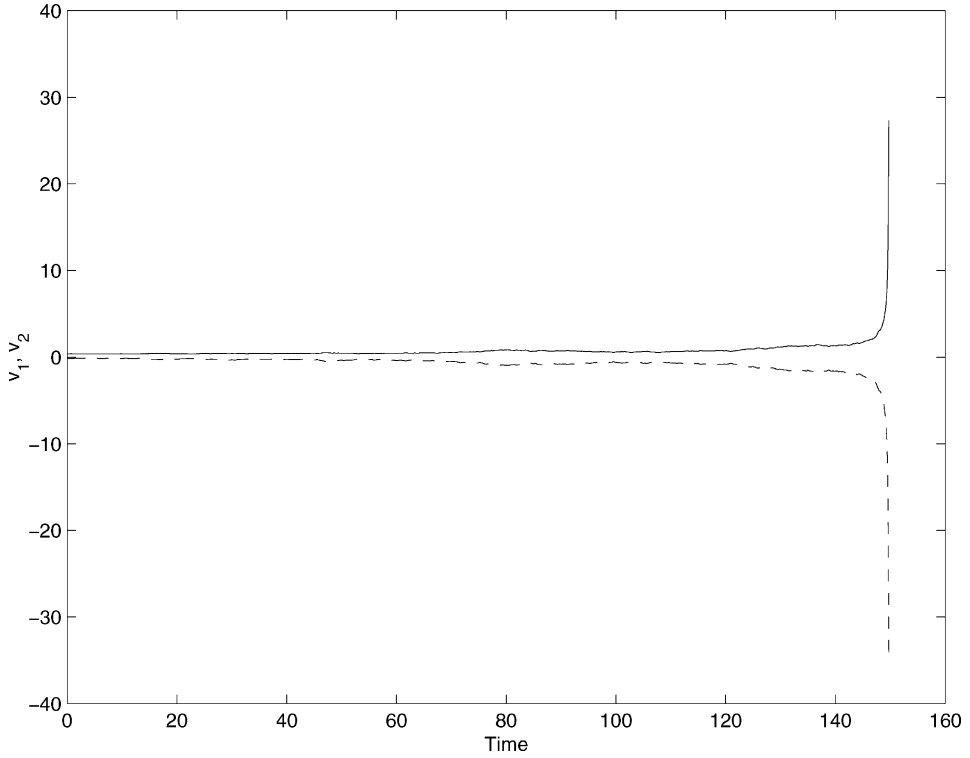

Fig. 10. Multiplicative triad system. The unaveraged processes $v_1(t)$, $v_2(t)$ in a situation with $B_1B_2 > 0$, $B_1B_3 > 0$ where no stationary distribution exists. Both processes grow unboundedly very fast in time.

is given in (18) with the C_j's given by (39), (41) and (42) or (43). The only additional difficulty with (46) is that the change of variable leading to this non-dimensional system of equations also depends of the initial condition through the values of M_{12}^0 and $\mathrm{sgn}(v_1^0)$ or $\mathrm{sgn}(v_2^0)$. Consistency with (28) thus leads to some additional constraint on the initial condition for (46) which can be satisfied, e.g. by taking the initial condition for (46) at the tips of the ellipse or the hyperbola on which the motion of v_1, v_2 is restricted, i.e.

$$v_1^0 = 1, \quad v_2^0 = 0 \ \text{ if } \ B_1B_2 < 0, \quad v_1^0 = \left(1 + \frac{|B_3B_2|\sigma_3^2}{2|B_1M_{12}^0|}\right)^{-1/2}, \quad v_2^0 = 0 \ \text{ if } \ B_1B_2 > 0 \ \text{ and } \ B_1M_{12}^0 < 0,$$
$$v_1^0 = 0, \quad v_2^0 = \left(1 + \frac{|B_3B_1|\sigma_3^2}{2|B_2M_{12}^0|}\right)^{-1/2} \ \text{ if } \ B_1B_2 > 0 \ \text{ and } \ B_1M_{12}^0 > 0. \tag{48}$$

From now on we work with (46) unless explicitly stated otherwise. The initial condition for (46) can be taken as

$$v_1^0 = 1, \quad v_2^0 = 0 \ \text{ if } \ \bar{b}_1\bar{b}_2 < 0, \quad v_1^0 = \delta, \quad v_2^0 = 0 \ \text{ if } \ \bar{b}_1\bar{b}_2 > 0 \ \text{ and } \ \bar{b}_1 > 0,$$
$$v_1^0 = 0, \quad v_2^0 = \delta \ \text{ if } \ \bar{b}_1\bar{b}_2 > 0 \ \text{ and } \ \bar{b}_1 < 0 \tag{49}$$

with $\delta \in [-1, 1]$, and the solution of (46) with the initial condition in (49) defines a four parameter family, $(\bar{b}_1, \bar{b}_2, \bar{b}_3, \varepsilon)$, on the ellipses, and a five parameter family, $(\bar{b}_1, \bar{b}_2, \bar{b}_3, \varepsilon, \delta)$, on the hyperbola. Here recall that one of the $\bar{b}_j$ is ± 1 by construction, the other two take values in $[-1, 1]$, $\delta \in (0, 1]$, and $\varepsilon > 0$ is arbitrary.

2.2.3. Mode elimination

As explained in the additive triad case, the method for mode elimination in [6] applies rigorously if $\varepsilon \ll 1$. Here, it corresponds to situations where the time-scale of the mode v_3 is much smaller than the time-scales of the modes v_1, v_2, since at statistical steady state (46) gives to leading order in $\varepsilon \ll 1$

$$\langle v_3(t+s)v_3(s)\rangle = \mathrm{e}^{-|t|/\varepsilon}, \tag{50}$$

whereas the time-correlation functions for v_1, v_2 will decay on a time-scale of the order of ε^{-1} (see (52)).

As extensively developed in [6] by the authors, the mode elimination procedure is actually simpler in the multiplicative triad case because the equation for v_3 in (16) can be solved explicitly as

$$v_3(t) = v_3^0\,\mathrm{e}^{-t/\varepsilon} + \bar{b}_3\int_0^t \mathrm{e}^{-(t-s)/\varepsilon}v_1(s)v_2(s)\,\mathrm{d}s + \sqrt{\frac{2}{\varepsilon}}\int_0^t \mathrm{e}^{-(t-s)/\varepsilon}\,\mathrm{d}W_3(s). \tag{51}$$

Inserting this expression in the equations for v_1, v_2 in (46) and performing asymptotic expansion in $\varepsilon \ll 1$ gives to leading order the following equations for v_1, v_2 alone:

$$\frac{\mathrm{d}v_1}{\mathrm{d}t} = \varepsilon\bar{b}_1\bar{b}_2v_1 + \varepsilon\bar{b}_3\bar{b}_1v_2^2v_1 + \sqrt{2\varepsilon}\bar{b}_1v_2\dot{W}(t), \qquad \frac{\mathrm{d}v_2}{\mathrm{d}t} = \varepsilon\bar{b}_1\bar{b}_2v_2 + \varepsilon\bar{b}_3\bar{b}_2v_1^2v_2 + \sqrt{2\varepsilon}\bar{b}_2v_1\dot{W}(t). \tag{52}$$

The initial condition for these equations is given in (49). Coarse-graining time as $t \to t/\varepsilon$ in this equation amounts to setting $\varepsilon = 1$, and in fact the solution of (52) converges to the solution of the first two equations in (46) as $\varepsilon \to 0$ in the coarse-grained time-scale t/ε.

In the original variables, (52) reads

$$\frac{\mathrm{d}v_1}{\mathrm{d}t} = \frac{\sigma_3^2B_1B_2}{\gamma_3^2}v_1 + \frac{B_1B_3}{\gamma_3}v_2^2v_1 + \frac{\sigma_3B_1}{\gamma_3}v_2\dot{W}(t), \qquad \frac{\mathrm{d}v_2}{\mathrm{d}t} = \frac{\sigma_3^2B_1B_2}{\gamma_3^2}v_2 + \frac{B_2B_3}{\gamma_3}v_1^2v_2 + \frac{\sigma_3B_2}{\gamma_3}v_1\dot{W}(t). \tag{53}$$

These equations conserve the Manley–Rowe relation M_{12}, (29), in each realization. (Thus, (53) could be further reduced into a single equation for v_1, say, by using the constraint $M_{12} = M_{12}^0$.) Furthermore, it can be checked by direct verification that the density in (35) projected in the (v_1, v_2) is the density of the stationary distribution associated with (52). Thus, we have full consistency between the original triad system in (28) and (46) and the reduced equations in (52) and (53). As in the additive case, if the parameters are such that there is no stationary distribution for the dynamics in (28), then (53) remains valid locally in time provided that the initial ε is small enough.

2.2.4. Numerical simulations

We now compare the statistics of the slow modes v_1 and v_2 predicted either from (52) or from the non-dimensional form of the triad equations in (46). Since the solution of the reduced equations in (52) is not available, we use numerical methods for both the equations in (28) and (52). We perform the simulations with

$$\bar{b}_1 = 0.4384, \qquad \bar{b}_2 = 0.5616, \qquad \bar{b}_3 = -1, \qquad \delta = 0.7254 \tag{54}$$

for the more difficult case in which the motion is restricted on a hyperbola and the stationary distribution exists, and consider four values of ε:

$$\varepsilon = 0.1, 0.2, 0.4, 1. \tag{55}$$

The triad equations in (28) are integrated as in the additive case. The reduced equations for the v_1 and v_2 in (52) are integrated by a split step algorithm utilizing the combination of the fourth-order Runge–Kutta algorithm and the "exact solution" formula for the multiplicative noise part of the equations. The exact solution of the stochastic

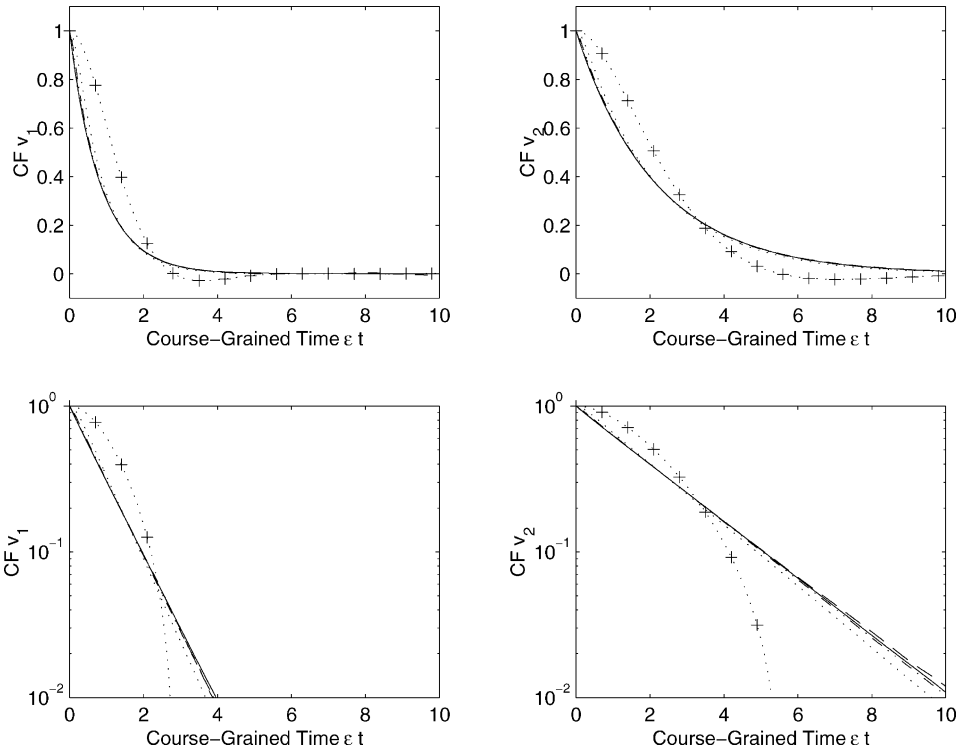

Fig. 11. Multiplicative triad system. Comparison of the correlation functions for v_1 and v_2 for the multiplicative triad equations in (46) and the reduced equations in (52) with different values of ε. Solid line: reduced equations; dashed line: $\varepsilon = 0.1$; dot-dashed line: $\varepsilon = 0.2$; dotted line: $\varepsilon = 0.4$; dotted-plus line: $\varepsilon = 1$.

part for the right-hand side of (52) can be obtained in closed form as an integral over white-noise (see [17]). Similar to the Ornstein–Uhlenbeck process discussed earlier, the numerical scheme for the stochastic terms is a suitable discretization of the exact solution formula. Statistics are obtained by time-averaging in this ergodic system.

In Fig. 11, we first compare the time-correlation functions of (v_1, v_2) predicted either from (28) and (52). We obtain excellent agreement between the predictions of the triad equations and effective equations for all values of ε including $\varepsilon = 0.4$, except for the very large value $\varepsilon = 1$.

We also checked higher order statistics of the resolved modes v_1, v_2. For simplicity we focus on mode v_2 which, unlike v_1, has zero mean for the range of parameter which we consider. As in the additive case, we used

$$K_2(t) = \frac{\langle v_2^2(t+s)v_2^2(s)\rangle}{\langle v_2^2\rangle^2 + 2\langle v_2(t+s)v_2(t)\rangle^2}, \tag{56}$$

which represents how the energy in mode v_2 correlated with itself. From the densities in (36) we know that the process is already non-Gaussian on the stationary distribution (one-time statistics), i.e. $K_2(0) \neq 1$. The results presented in Fig. 12 show that the departure from Gaussianity is even more pronounced for two times averaged quantities such as $K_2(t)$ for $t > 0$. The reduced equations in (46) reproduce this non-Gaussian behavior very accurately for all values of ε, except $\varepsilon = 1$. It should be stressed that it is essential that the reduced equations in (52) are of multiplicative type in order to reproduce such departure from Gaussianity. In particular, it *cannot* be

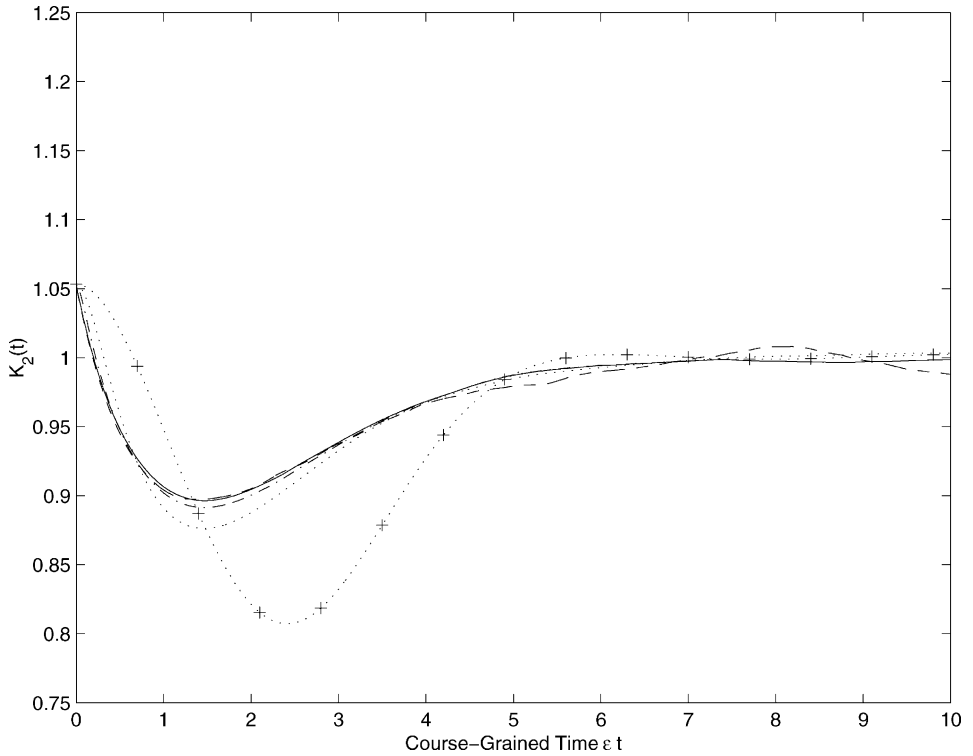

Fig. 12. Multiplicative triad system. The two-time fourth-order moment $K_2(t)$ defined in (56). Solid line: reduced equations; dashed line: $\varepsilon = 0.1$; dot-dashed line: $\varepsilon = 0.2$; dotted line: $\varepsilon = 0.4$; dotted-plus line: $\varepsilon = 1$.

reproduced by a linear Langevin equation of Ornstein–Uhlenbeck type (compare Figs. 5 and 12) which is the form assumed in a posteriori regression fitting procedures of the second-order correlations in Fig. 11.

3. Stochastic modeling in systems with many degrees of freedom

The truncated Burgers–Hopf system was introduced in [15,16] by two of the authors as a simple test model for various statistical theories and stochastic modeling procedures. The truncated Burgers–Hopf system is defined by the following system of nonlinear ordinary differential equations for the complex modes $\hat{u}_k$, satisfying $\hat{u}_k^* = \hat{u}_{-k}$:

$$\frac{\mathrm{d}\hat{u}_k}{\mathrm{d}t} = -\frac{\mathrm{i}k}{2} \sum_{\substack{k+p+q=0 \\ |p|,|q|\le\Lambda}} \hat{u}_p^* \hat{u}_q^*, \quad 1 \le k \le \Lambda, \quad \Lambda \in \mathbb{N}. \tag{57}$$

The truncated Burgers–Hopf system displays features in common with vastly more complicated systems: it is deterministic but chaotic and mixing, it is ergodic on suitably defined equi-energy surfaces, and the time correlations for the various degrees of freedom are different but obey a simple scaling law. These properties make the truncated Burgers–Hopf system an ideal candidate for a stochastic heat bath.

In this paper we consider a simple extension of the truncated Burgers–Hopf system obtained by coupling the equations in (57) to one or two additional modes. The coupled truncated Burgers–Hopf system is constructed in such a way that there is a free parameter in the problem which controls the time-scale for the additional modes.

The coupling can also be adjusted in various ways so that the nonlinear interaction between the additional modes and the Burgers bath be of additive type, multiplicative type, or both types at once. Here we use the terminology introduced for the triad systems. In this way the coupled truncated Burgers–Hopf system provides a simple but highly non-trivial test case for the mode elimination procedure developed in [5,6] which yields a closed system of equations for the additional modes alone.

After recalling the main properties of the system in (57) we shall investigate the coupled truncated Burgers–Hopf system in various settings. First, in Section 3.2, we shall consider a coupled system with one additional mode for which the reduced equation is of additive type. In Section 3.2 we discuss in detail our stochastic modeling assumption, which leads us to the issue of stochastic consistency. In particular, we show how to determine the various parameters entering the stochastic model. We also give both an empirical and an a priori criterion to quantify the mode elimination procedure (i.e. we obtain what is the appropriate ε for the model). These results are used in Sections 3.3 and 3.4 where we discuss the coupled truncated Burgers–Hopf system in two different settings, one of multiplicative type and one which combines both additive and multiplicative types.

3.1. The truncated Burgers–Hopf system

The model is defined as a finite-dimensional Fourier Galerkin truncation of the inviscid Burgers–Hopf equations on the periodic $[0, 2\pi]$ domain

$$(u_\Lambda)_t + \tfrac{1}{2} P_\Lambda (u_\Lambda^2)_x = 0, \tag{58}$$

where P_Λ, $\Lambda \in \mathbb{N}$, is the projection operator in Fourier space

$$P_\Lambda f(x) = f_\Lambda(x) = \sum_{k \le \Lambda} \hat{f}_k \, \mathrm{e}^{\mathrm{i}kx}, \quad \hat{f}_k = \frac{1}{2\pi} \int_0^{2\pi} f(x) \, \mathrm{e}^{-\mathrm{i}kx} \, \mathrm{d}x. \tag{59}$$

In terms of the Fourier modes $\hat{u}_k$,

$$u_\Lambda(x) = \sum_{k \le \Lambda} \hat{u}_k \, \mathrm{e}^{\mathrm{i}kx}, \tag{60}$$

the equations in (58) reduce to (57). The equations in (57) satisfy the Liouville property and conserve the momentum

$$M = \frac{1}{2\pi} \int_0^{2\pi} u_\Lambda \, \mathrm{d}x = \hat{u}_0, \tag{61}$$

and the energy

$$E = \frac{1}{4\pi} \int_0^{2\pi} u_\Lambda^2 \, \mathrm{d}x = \frac{1}{2} |\hat{u}_0|^2 + \sum_{k=1}^{\Lambda} |\hat{u}_k|^2. \tag{62}$$

The momentum constraint is trivial and without loss of generality we consider solutions with $M = \hat{u}_0 = 0$. In addition to the conserved quantities in (61) and (62) the discrete analog

$$H = \int_0^{2\pi} u_\Lambda^3 \, \mathrm{d}x, \tag{63}$$

is also conserved [16,18]. For a typical initial condition, $H \approx 0$ for large Λ by the central limit theorem. As a result the conservation of H does not affect the statistical behavior of the solutions for most initial data if Λ is large enough (for a precise discussion of this issue, see [18]).

The Liouville property together with the conservation of energy implies that the canonical Gibbs measure with density

$$p_\beta = Z^{-1} \exp\left(-\beta \sum_{k=1}^{\Lambda} |u_k|^2\right), \quad \beta > 0 \tag{64}$$

is a stationary distribution for the dynamics in (57). In fact, the numerical results reported in [15,16] suggest that the Gibbs measure is the appropriate (at fixed β) stationary distribution for (57), at least for large enough values of Λ such as $\Lambda = 50$ utilized here, with a very fast convergence in Λ. More precisely, for almost all initial conditions, the dynamics in (57) will eventually span (64) in the sense that

$$\frac{1}{T}\int_0^T f(y_{i_1}(t), z_{i_1}(t), \ldots, y_{i'_\Lambda}(t), z_{i'_\Lambda}(t))\,\mathrm{d}t \approx \int_{\mathbf{R}^{2\Lambda}} f(y_{i_1}, z_{i_1}, \ldots, y_{i'_\Lambda}, z_{i'_\Lambda}) p_\beta \,\mathrm{d}y_1\,\mathrm{d}z_1, \ldots, \mathrm{d}y_\Lambda\,\mathrm{d}z_\Lambda, \tag{65}$$

where $\hat{u}_k = y_k + \mathrm{i}z_k$, and $\{y_{i_1}, z_{i_1}, \ldots, y_{i'_\Lambda}, z_{i'_\Lambda}\}$ is an arbitrary subset of the original variables with $\Lambda' \ll \Lambda$. For a given value E_0 of the energy in (62) computed from the initial conditions, β is given by

$$\beta = \frac{\Lambda}{E_0}. \tag{66}$$

Thus, the canonical Gibbs measure predicts equipartition of energy among all modes $1 \le k \le \Lambda$ with

$$\mathrm{cov}(\hat{u}_k) = \beta^{-1} = \frac{E_0}{\Lambda}. \tag{67}$$

These statistical predictions were confirmed in [15,16] with surprising accuracy. Furthermore, the model in (57) has a very high rate of mixing and achieves the statistical steady state rather quickly.

A simple dimensional argument for the decorrelation rate of the modes $\hat{u}_k(t)$ was also presented and confirmed numerically in [15,16]. Under the assumption that the energy per mode, $E_0/\Lambda = \beta^{-1}$, with units length^2/time^2, and the wavenumber, k, with units length^{-1}, are the only relevant dimensional parameters for mode k, it follows that this mode must decorrelate on a time-scale proportional to the eddy turnover time defined as

$$T_k = \frac{C_0\sqrt{\beta}}{k}, \quad 1 \le k \le \Lambda, \tag{68}$$

where C_0 is a universal constant of proportionality independent of β and k. Thus, we expect

$$\int_0^\infty \langle \hat{u}_k(t+s)\hat{u}_k^*(s)\rangle\,\mathrm{d}t = \beta^{-1}T_k = \frac{C_0}{k\sqrt{\beta}}. \tag{69}$$

The numerical experiments [15,16] confirm the scaling in (69), with a constant of proportionality, C_0, only weakly dependent on the size of the truncation, Λ. It was observed that, to numerical accuracy, the correlation functions for the real and imaginary parts of $\hat{u}_k$, $y_k = \mathrm{Re}\,\hat{u}_k$, and $z_k = \mathrm{Im}\,\hat{u}_k$, are equal

$$\langle y_k(t+s)y_k(s)\rangle = \langle z_k(t+s)z_k(s)\rangle, \tag{70}$$

while the cross-correlation functions between y_k and z_k are zero,

$$\langle y_k(t+s)z_k(s)\rangle = 0. \tag{71}$$

3.2. Coupled truncated Burgers–Hopf system with one additional mode: additive case

Now we shall consider the following extension of the truncated Burgers–Hopf system ($1 \le k, |p|, |q| \le \Lambda$):

$$\frac{\mathrm{d}x_1}{\mathrm{d}t} = \lambda \sum_k b_k^{1|yz} y_k z_k, \qquad \frac{\mathrm{d}y_k}{\mathrm{d}t} = -\mathrm{Re}\,\frac{\mathrm{i}k}{2} \sum_{p+q+k=0} \hat{u}_p^* \hat{u}_q^* + \lambda b_k^{y|1z} x_1 z_k,$$
$$\frac{\mathrm{d}z_k}{\mathrm{d}t} = -\mathrm{Im}\,\frac{\mathrm{i}k}{2} \sum_{p+q+k=0} \hat{u}_p^* \hat{u}_q^* + \lambda b_k^{z|1y} x_1 y_k, \tag{72}$$

where $u_k = y_k + \mathrm{i}z_k$. The interaction coefficients $b_k^{\cdot|\cdot\cdot}$ are of order 1 and satisfy

$$b_k^{1|yz} + b_k^{y|1z} + b_k^{z|1y} = 0. \tag{73}$$

The parameter λ is a measure of the strength of coupling between the additional mode, x_1, and the Burgers bath (y_k, z_k). For $\lambda = 0$, the system in (72) reduces to the truncated Burgers–Hopf system in (57). For $\lambda \neq 0$, one can think of mode x_1 as being driven by the Burgers bath. We will derive a closed stochastic differential equation for x_1 alone by suitable elimination of the bath modes (y_k, z_k) using the theory from Majda et al. [5,6]. Note that the nonlinear terms containing any given triple, (x_1, y_k, z_k), k fixed, in the right-hand side of the equations in (72) are of the same type as in the additive triad model. Thus we can expect that the reduced equation for x_1 alone obtained from (72) will be linear in x_1 with an additive noise. This is confirmed below.

Throughout this section, we shall consider (72) in the regime

$$\Lambda = 50, \qquad \lambda = 4 \tag{74}$$

with the first five interaction coefficients non-zero and picked at random as listed in Table 1. These coefficients were generated randomly in the range $[-1, 1]$ with the constraint that they satisfy (73). The initial conditions were taken such that the parameter β, measuring the energy per mode and defined through

$$\frac{1}{2\beta} = \frac{E_0}{1+2\Lambda}, \quad E_0 = x_1^2(0) + \sum_{k=1}^{\Lambda} (y_k^2(0) + z_k^2(0)), \tag{75}$$

has value

$$\beta = 50. \tag{76}$$

We show below that the energy, E_0, is conserved in time for (72), so that β is well defined independent of time. In the numerical simulations, the equations in (72) are integrated using a pseudo-spectral method for the evaluation of the nonlinear terms of the Burgers bath and a fourth-order Runge–Kutta scheme for time-stepping. All the statistics in the deterministic system are computed through time-averaging in a standard fashion [15,16].

Table 1
Coupled truncated Burgers–Hopf system: additive case. The interaction coefficients

k	$b_k^{1\|yz}$	$b_k^{y\|1z}$	$b_k^{z\|1y}$
1	0.2810	−0.6675	0.3865
2	0.3923	−0.9356	0.5433
3	0.3953	−0.6975	0.3023
4	0.3523	−0.6520	0.2997
5	0.5245	−0.8272	0.3027

Unlike the triad systems, the system in (72) is deterministic. To proceed, we shall approximate the system in (72) by a stochastic model following the method developed in [5,6]. We will discuss in detail the stochastic consistency between the original system and the stochastic model. Next, we determine the small parameter ε in terms of the other parameters in the system. Finally, we perform mode elimination on the stochastic model and obtain a closed equation for the mode x_1 alone. Before doing all this, though, we determine some properties of (72).

3.2.1. Stationary distribution

Due to the constraint (73) on the coupling coefficients $b_k^{\cdot|\cdot\cdot}$, the system in (72) conserves the energy

$$E = x_1^2 + \sum_{k=1}^{\Lambda} |u_k|^2 = x_1^2 + \sum_{k=1}^{\Lambda} (y_k^2 + z_k^2). \tag{77}$$

(The coupling destroys the other invariant M, and H, see (61) and (63).) It can also be checked by direct calculation that the system in (72) satisfies the Liouville property

$$0 = \frac{\partial F_{x_1}}{\partial x_1} + \sum_{k=1}^{\Lambda} \left(\frac{\partial F_{y_k}}{\partial y_k} + \frac{\partial F_{z_k}}{\partial z_k} \right), \tag{78}$$

where $F_{x_1}, \ldots$ denote the respective right-hand sides of the equations in (72). The conservation of energy together with the Liouville property imply that the Gibbs measure with density

$$p_\beta = Z^{-1} \exp(-\beta E) = Z^{-1} \exp\left(-\beta \left(x_1^2 + \sum_{k=1}^{\Lambda} (y_k^2 + z_k^2) \right) \right), \tag{79}$$

is a stationary distribution for the dynamics in (72). In fact, the numerical results support that, for a large number of degrees of freedom like $\Lambda = 50$, (79) is the density of the unique (for fixed energy) stationary distribution for the system in (72), i.e. for almost all initial conditions for (72), the dynamics will eventually span (79) similarly as in (65). The density in (79) implies equipartition of energy among mode x_1 and the bath variables (y_k, z_k)

$$\mathrm{cov}(x_1) = \mathrm{cov}(y_k) = \mathrm{cov}(z_k) = \frac{1}{2\beta}, \tag{80}$$

and the parameter β is uniquely determined by the energy in (77) computed on the initial condition, E_0, through (75). With the above parameters as in [15,16], the numerical simulations strongly confirm (79) and (80). The numerical values for the first few moments of x_1 which are consistent with these predictions are given in Table 2.

It is worth noting that the parameter λ in (72) does not affect the one-time statistical properties of the system. Of course, this parameter will influence the two-time statistics, as investigated below.

3.2.2. Stochastic modeling and stochastic consistency

As mentioned before, the mode elimination technique developed in [5,6] applies to stochastic differential equations, not deterministic systems as in (72). Thus, in a first step we need to approximate (72) by some stochastic

Table 2
Coupled truncated Burgers–Hopf system: additive case. One point statistics for mode x_1

	Stat Mech	DNS
$\langle x_1 \rangle$	0	0.0015
$\langle x_1^2 \rangle$	0.01	0.010025
$\langle x_1^4 \rangle$	0.0003	0.0003004

model. With x_1 declared as the only resolved mode, the strategy in [5,6] is to replace the nonlinear self-interaction terms in the equation for the unresolved modes, (y_k, z_k), by some stochastic model. Specifically, we shall make the following stochastic modeling assumption (also used in Sections 3.3 and 3.4):

$$\frac{\mathrm{i}k}{2} \sum_{p+q+k=0} \hat{u}_p^* \hat{u}_q^* \approx -\gamma_k u_k + \sigma_k (\dot{W}_k^y(t) + \mathrm{i}\dot{W}_k^z(t)), \tag{81}$$

where $W_k^y(t)$, $W_k^z(t)$ are independent Wiener processes. Thus, we replace the original system in (72) by the stochastic model

$$\frac{\mathrm{d}x_1}{\mathrm{d}t} = \lambda \sum_k b_k^{1|yz} y_k z_k, \qquad \frac{\mathrm{d}y_k}{\mathrm{d}t} = \lambda b_k^{y|1z} x_1 z_k - \gamma_k y_k + \sigma_k \dot{W}_k^y(t),$$
$$\frac{\mathrm{d}z_k}{\mathrm{d}t} = \lambda b_k^{z|1y} x_1 y_k - \gamma_k z_k + \sigma_k \dot{W}_k^z(t). \tag{82}$$

Note that this stochastic model might already involve a smaller number of equations since we only need to consider those (y_k, z_k) such that $b_k^{1|yz} \neq 0$ (recall that though $\Lambda = 50$, we took $b_k^{1|yz} \neq 0$ for the first five modes only, see Table 1).

The parameters γ_k, σ_k must be chosen so as to optimize stochastic consistency between the approximated model in (82) and the original coupled truncated Burgers–Hopf system in (72). In fact, there is a first obvious criterion for consistency which fixes the ratio σ_k^2/γ_k: the stationary distribution for (82) will be exactly (64) if

$$\frac{\sigma_k^2}{\gamma_k} = \frac{1}{\beta}. \tag{83}$$

Thus it only remains to determine γ_k (say), and we now discuss this issue in some detail using numerical experiments. The stochastic model in (82) was integrated using time-splitting with a second-order Runge–Kutta algorithm for the nonlinear coupling terms and the "exact solution" formula for the Ornstein–Uhlenbeck process for the damping and forcing terms in (82).

There are various different strategies to determine γ_k, which are all based on optimizing the matching between the time-correlation functions of the unresolved modes

$$\langle y_k(t+s) y_k(s) \rangle = \langle z_k(t+s) z_k(s) \rangle, \tag{84}$$

predicted by the original system in (72) and by the stochastic model in (82). (We shall also use these strategies in Sections 3.3 and 3.4 for other variants of the coupled truncated Burgers–Hopf system.) A common difficulty faced by all the strategies given below and others in the literature (see the applied references in [6]), is that it is not possible to reproduce all the details of the actual correlation functions for the original model in (72) by such a first-order Markov model. We can only expect to capture some coarse-grained information about these functions, and the natural choice in these first-order Markov models is to approximate the actual correlation functions by exponentials

$$\exp(-\gamma_k^{\mathrm{dns}} |t|), \tag{85}$$

where γ_k^{dns} is the area below $\langle y_k(t+s) y_k(s) \rangle$, $\langle z_k(t+s) z_k(s) \rangle$ normalized by 2β:

$$\gamma_k^{\mathrm{dns}} = (2\beta \times \text{area under the actual correlation function of mode } k)^{-1}. \tag{86}$$

The values of γ_k^{dns} are given in Table 3 and the functions $\exp(-\gamma_k^{\mathrm{dns}}|t|)/2\beta$ and the actual correlation functions are compared in Fig. 13. We now pick the γ_k in the stochastic model so as to optimize consistency with (85) using one of the following three different procedures:

Table 3
Coupled truncated Burgers–Hopf system: additive case. Comparison between the $\gamma_k^{\rm scal}$ obtained from the scaling law in (87), the $\gamma_k^{\rm dns}$ obtained from (86), and the adjusted $\gamma_k^{\rm adj}$ used in the stochastic model with procedure 2

k	$\gamma_k^{\rm scal}$	$\gamma_k^{\rm dns}$	$\gamma_k^{\rm adj}$
1	0.7107	0.7147	0.6027
2	1.4213	1.4160	1.1543
3	2.1320	2.0637	2.0637
4	2.8427	2.7069	2.7069
5	3.5534	3.3176	3.3176

(P1) The most a priori strategy consists in using the scaling law in (68) for the uncoupled truncated Burgers–Hopf dynamics and identify γ_k with

$$\gamma_k^{\rm scal} = T_k^{-1} = \frac{C_1 k}{\sqrt{\beta}}. \tag{87}$$

Here $C_1 = 1/C_0$ is the only numerical constant left to determine; this can be done once and for all, e.g., by measuring $\gamma_{k=1}$ from the numerical simulations for the uncoupled truncated Burgers–Hopf system. For the parameters used in the simulations this gives

$$C_1 = 5.03, \tag{88}$$

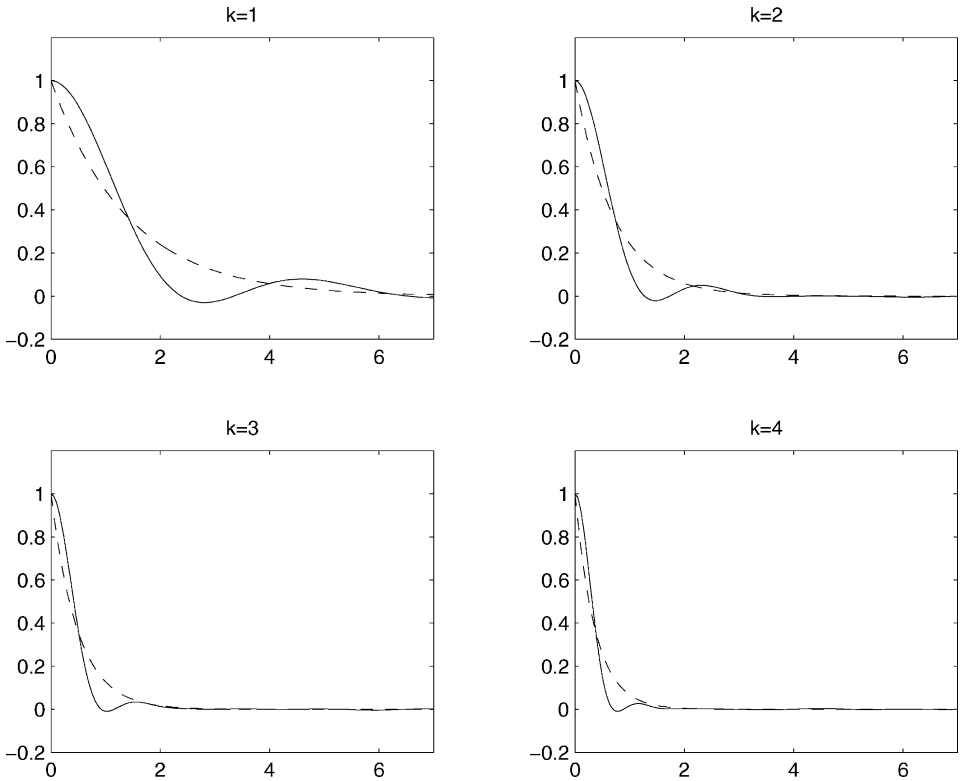

Fig. 13. Coupled truncated Burgers–Hopf system: additive case. Comparison between the actual correlation functions for modes (y_k, z_k) from the original system in (72) (full line) and the functions $\exp(-\gamma_k^{\rm dns}|t|)/2\beta$ (dashed line).

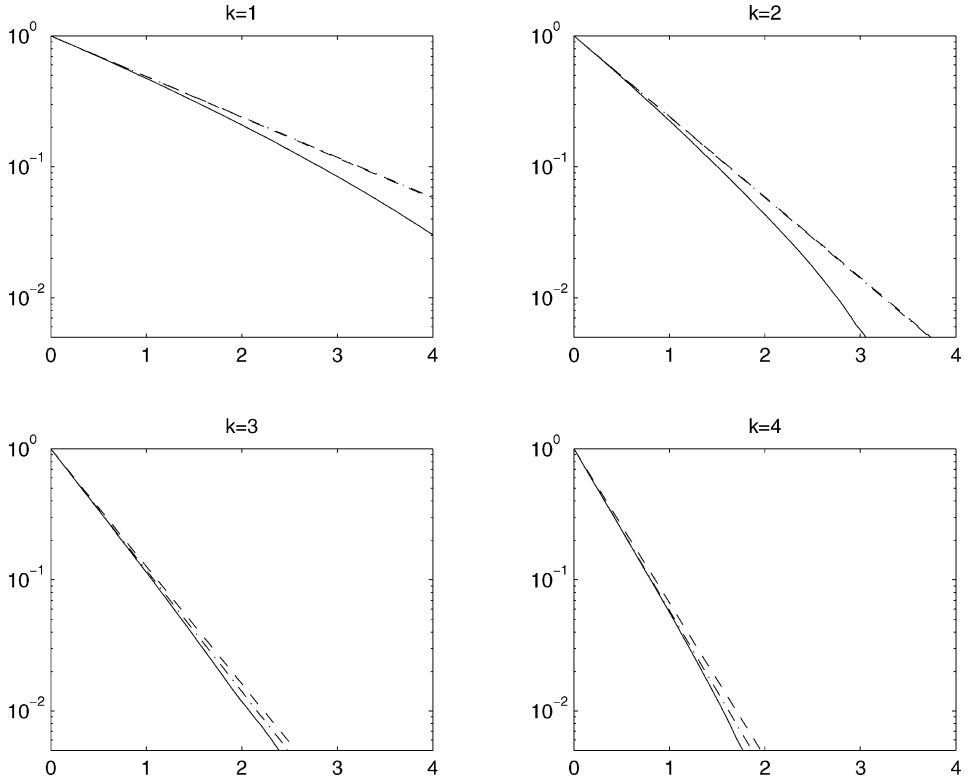

Fig. 14. Coupled truncated Burgers–Hopf system: additive case. Comparison between the correlation functions obtained from the stochastic model in (82) with $\gamma_k = \gamma_k^{\mathrm{scal}}$ (full line), the functions $\exp(-\gamma_k^{\mathrm{dns}}|t|)/2\beta$ (dashed line), $\exp(-\gamma_k^{\mathrm{scal}}|t|)/2\beta$ (dot-dashed line).

and the corresponding γ_k^{scal} are listed in Table 3. The underlying assumption behind (87) is that the coupling with x_1 in both (72) and (82) does not affect very much the correlation functions of the unresolved modes (y_k, z_k). As explained in Section 3.2.3, this is justified in the range of parameters where mode elimination applies because to leading order in the appropriate ε there is separation of time-scales between the fast unresolved modes (y_k, z_k) and the slow resolved mode x_1. Thus, in first approximation the fast dynamics on which the unresolved modes decorrelate is governed solely by the nonlinear self-interactions between y_k and z_k's in (72) or, equivalently through the stochastic modeling assumption in (81), by the forcing and damping terms in (82). In Fig. 14, we compare on the logarithmic scale the functions $\exp(-\gamma_k^{\mathrm{dns}}|t|)/2\beta$, $\exp(-\gamma_k^{\mathrm{scal}}|t|)/2\beta$, and the correlation functions for (y_k, z_k) obtained by integration of the stochastic model in (82) with $\gamma_k = \gamma_k^{\mathrm{scal}}$. This figure clearly shows the potential problem with procedure P1. The coupling with x_1 might not be completely negligible and may actually change the correlation functions. Fig. 14 shows that the decay rates for the correlation functions predicted by both the original system and the stochastic model are not γ_k^{scal} in the example at hand. The stochastic model tends to overestimate the decay rate γ_k^{scal}, especially for the first two modes with $k = 1, 2$.

(P2) We show in Section 3.2.3 that when the parameters are such that mode elimination is justified, to leading order in the appropriate ε the correlation functions of the stochastic model in (82) display an exponential decay given by

$$\langle y_k(t+s)y_k(s)\rangle = \langle z_k(t+s)z_k(s)\rangle \approx \frac{\mathrm{e}^{-\gamma_k|t|}}{2\beta}. \tag{89}$$

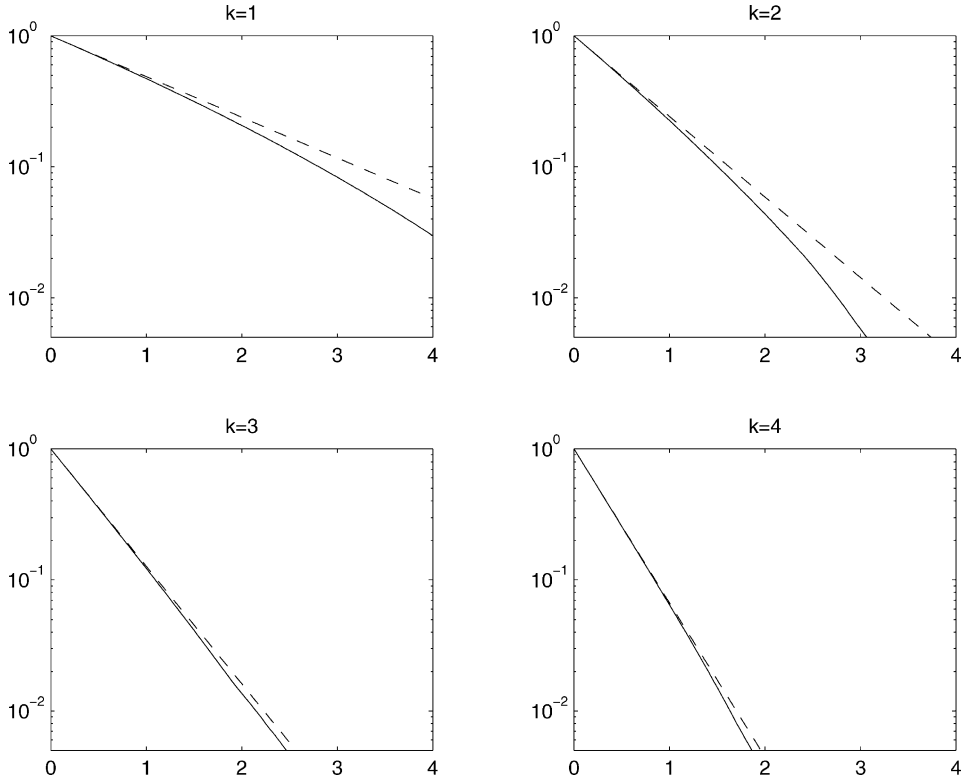

Fig. 15. Coupled truncated Burgers–Hopf system: additive case. Comparison between the functions $\exp(-\gamma_k^{\mathrm{dns}}|t|)/2\beta$ (dashed line) and the correlation functions obtained from the stochastic model in (82) with $\gamma_k = \gamma_k^{\mathrm{dns}}$ (full line).

This automatically leads us to identify γ_k with the γ_k^{dns} obtained from (86). The potential problem with procedure P2 is that the decay in (89) is only approximately true for the solution of the stochastic model in (82) (this is again due to coupling with mode x_1). This can be seen in Fig. 15 where we compare on the logarithm scale the functions $\exp(-\gamma_k^{\mathrm{dns}}|t|)/2\beta$ with the correlation functions for (y_k, z_k) obtained by integration of the stochastic model in (82) with $\gamma_k = \gamma_k^{\mathrm{dns}}$. Thus, for the example at hand, the stochastic model tends to overestimate the decay rate γ_k, especially for the first two modes with $k = 1, 2$. (Procedure P2 does in fact much better for the examples presented in Sections 3.3 and 3.4 where it give results as good as those obtained by the more refined procedure P3.)

(P3) Better results are expected if the γ_k's are picked in such a way that the correlation functions for the unresolved modes solution of the stochastic model in (82) reproduce the functions $\exp(-\gamma_k^{\mathrm{dns}}|t|)/2\beta$ as closely as possible. As we just explained, generally this amounts to taking $\gamma_k = \gamma_k^{\mathrm{adj}} \neq \gamma_k^{\mathrm{dns}}$. The values for the γ_k^{adj} given in Table 3 were used in the stochastic model to obtain the correlation functions depicted in Fig. 16. The agreement is now quasi-perfect for all the modes, though we only adjusted the value of γ_k for the first two modes, $k = 1, 2$.

Note that none of the procedures P1–P3 make adjustment at the level of the correlation function for the resolved mode, x_1. In this sense they are all a priori procedures. How good the stochastic model does (both for γ_k^{scal}, γ_k^{dns} and γ_k^{adj}) at the level of the resolved mode (here x_1) will be discussed below in Section 3.2.4 about mode elimination (see also Sections 3.3.3 and 3.4.2 for the coupled truncated Burgers system in different settings). Notice that procedures P1–P3 are actually much more a priori than what disciplinary people in, say, the atmosphere/ocean

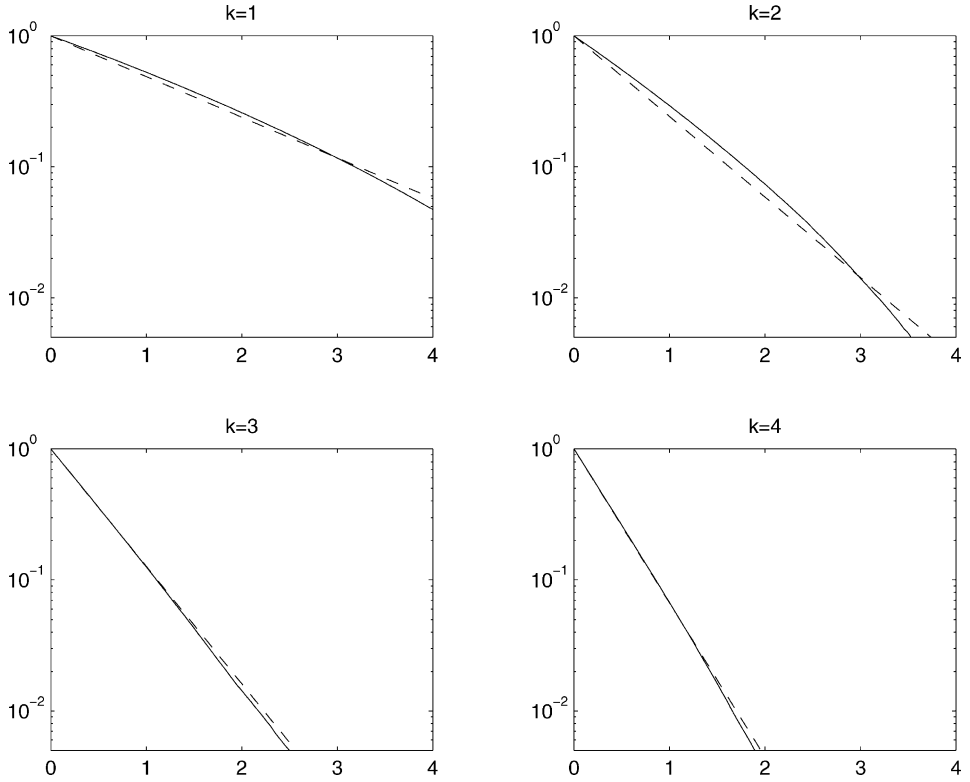

Fig. 16. Coupled truncated Burgers–Hopf system: additive case. Comparison between the correlation functions obtained from the stochastic model in (82) with $\gamma_k = \gamma_k^{\mathrm{adj}}$ (full line) and the functions $\exp(-\gamma_k^{\mathrm{dns}}|t|)/2\beta$ (dashed line).

science community might be willing to use in a stochastic modeling strategy (see the references in [6]). In fact, a purely empirical procedure, which we shall not discuss in this paper (see [19]) but is expected to give the best results, would be to forget altogether about consistency for the unresolved modes and simply require optimal matching for the correlation function of the resolved modes, x_1 here or (x_1, x_2) in Sections 3.3 and 3.4. In fact, this procedure gives truly excellent agreement between the reduced equations obtained by mode elimination and the coupled truncated Burgers–Hopf system in the various settings which we discuss, even in parameter regimes where the a priori procedures P1–P3 do not apply (i.e. even for ε of the order of 1) [19].

3.2.3. Determination of ε

In a last step before applying mode elimination to the stochastic model in (82) we determine when the procedure is supposed to apply or, in other words, what is ε. We give two ways to estimate ε. The first is empirical and pretty simple to obtain, though it might be fairly imprecise. The second estimate is a priori and more accurate though more complicated to obtain.

The empirical estimate for ε is obtained if one remembers that, in appropriate dimensionless units, the slower time-scale of the unresolved modes is of the order of ε, whereas the time-scale of the resolved mode is of the order ε^{-1} (see the discussion for the triad models and (92)). Thus, we can estimate

$$\varepsilon^{\mathrm{emp}} = \sqrt{\frac{\text{slowest time-scale of the unresolved modes, } y_k, z_k}{\text{time-scale of the resolved mode, } x_1}}. \tag{90}$$

Using this formula with the data from numerical simulations gives

$$\varepsilon^{\text{emp}} = 0.24.$$

Of course, the empirical estimate in (90) should be considered with care since it might miss a numerical factor (see (95)). For instance, applied to the additive triad system, the estimate in (90) gives $\varepsilon^{\text{emp}} = \varepsilon\sqrt{\gamma} \neq \varepsilon$ for small ε (we used (19) and (24), and γ is given by (21)).

For a more precise a priori estimate of ε, we proceed as in the triad systems and write the equations in (82) in appropriate non-dimensional variables. Specifically, we substitute

$$x_1 \to \frac{x_1}{\sqrt{2\beta}}, \qquad y_k \to \frac{y_k}{\sqrt{2\beta}}, \qquad z_k \to \frac{z_k}{\sqrt{2\beta}}, \qquad t \to \frac{t\sqrt{2\beta}}{\lambda}, \tag{91}$$

which amounts to rescaling all modes according to their (common) variance and time so that the nonlinear coupling terms between x_1 and (y_k, z_k) are all of order 1. Using (83), this leads to

$$\begin{aligned} &\frac{\mathrm{d}x_1}{\mathrm{d}t} = \sum_k b_k^{1|yz} y_k z_k, \qquad \frac{\mathrm{d}y_k}{\mathrm{d}t} = b_k^{y|1z} x_1 z_k - \frac{1}{\delta_k \varepsilon} y_k + \sqrt{\frac{2}{\delta_k \varepsilon}}\dot{W}_k^y(t), \\ &\frac{\mathrm{d}z_k}{\mathrm{d}t} = b_k^{z|1y} x_1 y_k - \frac{1}{\delta_k \varepsilon} z_k + \sqrt{\frac{2}{\delta_k \varepsilon}}\dot{W}_k^z(t), \end{aligned} \tag{92}$$

where using the generic property that the γ_k's increase with k (i.e. higher order mode decorrelate faster, see (68)), we define

$$\delta_{k=1} = 1, \qquad \delta_k = \frac{\gamma_{k=1}}{\gamma_k} \in (0, 1) \quad \text{for } |k| > 1. \tag{93}$$

Since all the terms but the forcing and damping terms in (92) are of order 1 or smaller (recall that the $b_k^{\cdot|\cdot\cdot}$ are of order 1 by construction), we identified ε by

$$\varepsilon = \frac{\lambda}{\gamma_{k=1}\sqrt{2\beta}}. \tag{94}$$

Using the parameters in the numerical simulations (see Section 3.2.2), (94) gives for $\gamma_{k=1} = \gamma_{k=1}^{\text{adj}}$

$$\varepsilon = 0.63.$$

This estimate is in fair agreement with the empirical estimate from (90). In fact, using (97), we see that

$$\varepsilon^{\text{emp}} \approx \varepsilon \sqrt{\sum_k \delta_k (b_k^{1|yz})^2}, \tag{95}$$

which accounts indeed for the discrepancy between (90) and (94). Note also that the estimate in (94) gives a rather big value for ε in the example at hand: this should be kept in mind considering how good mode elimination does.

In what follows it will be more convenient to work with the dimensional equations in (72), and give the reduced equations obtained from (72) by mode elimination in their dimensional form as well. Thus, though no ε will be apparent in these equations, we will remember that ε is computed from (94).

3.2.4. Mode elimination

Following [6] a closed equation for x_1 alone can be obtained from the stochastic model in (82) by elimination of the unresolved variables (y_k, z_k), in the appropriate limit much in the same way as we obtained the reduced equation in (22) for the additive triad model. The equation is given by

$$\frac{\mathrm{d}x_1}{\mathrm{d}t} = -\gamma_1 x_1 + \sigma_1 \dot{W}(t) \tag{96}$$

with

$$\gamma_1 = \frac{\lambda^2}{4\beta} \sum_{k=1}^{\Lambda} \frac{(b_k^{1|yk})^2}{\gamma_k}, \qquad \sigma_1 = \sqrt{\frac{\gamma_1}{\beta}}. \tag{97}$$

Thus mode elimination predicts that x_1 is an Ornstein–Uhlenbeck process with a stationary distribution which always exists ($\gamma_1 > 0$) and coincides with the stationary distribution in (79) (projected in the x_1-space) of the original coupled truncated Burgers system in (72). We now further check the relevance of the reduced stochastic equations in (96) for the original dynamics in (72) by using the time-correlation function for x_1 and an indicator function for the departure from Gaussianity of this process.

The time-correlation function predicted from the reduced stochastic model in (96) is

$$\langle x_1(t+s)x_1(s)\rangle = \frac{\mathrm{e}^{-\gamma_1|t|}}{2\beta}. \tag{98}$$

We compare this function using γ_k^{scal}, γ_k^{dns}, or γ_k^{adj} in (97) (corresponding to procedures P1, P2, or P3) with the time-correlation functions obtained by numerical integration of both the original coupled truncated Burgers–Hopf system in (72) and the stochastic model in (82) using also γ_k^{scal}, γ_k^{dns}, or γ_k^{adj}. The simulations use the parameters listed in Section 3.2.2 and the results are presented in Fig. 17. Clearly, both the stochastic model and the reduced equation for x_1 in (96) reproduce rather well the actual correlation function for this mode, especially if the γ_k^{adj}'s are used. In fact, the analytical predictions for γ_1 from (97) using γ_k^{scal}, γ_k^{dns}, and γ_k^{adj} are, respectively

$$\gamma_1^{\mathrm{scal}} = 0.033, \qquad \gamma_1^{\mathrm{dns}} = 0.034, \qquad \gamma_1^{\mathrm{adj}} = 0.039, \tag{99}$$

while the value obtained from the original coupled truncated Burgers–Hopf system in (72) is

$$\gamma_1 = 0.04. \tag{100}$$

Notice that γ_1^{scal} is almost identical with γ_1^{dns}.

As a further check, we used the following indicator function for the departure from Gaussianity of x_1:

$$K_1(t) = \frac{\langle x_1^2(t+s)x_1^2(s)\rangle}{\langle x_1^2\rangle^2 + 2\langle x_1(t+s)x_1(s)\rangle^2}. \tag{101}$$

This quantity measures correlation in time of the energy, $x_1^2(t)$, in the mode: it is appropriately normalized so that $K_1(t) = 1$ for all time for a Gaussian x_1. The reduced equation in (96) precisely implies that x_1 is a Gaussian process, and Fig. 18 shows that this prediction is in very good agreement, within 5% accuracy, with the actual value for $K_1(t)$ obtained both from the original dynamics in (72) and the stochastic model in (82) (here we used $\gamma_k = \gamma_k^{\mathrm{adj}}$). In fact, systematic departures from Gaussianity which are well reproduced by the reduced equations will be observed in the examples considered in Sections 3.3 and 3.4, which involve multiplicative noises, and Fig. 18 should be compared with Figs. 22 and 26.

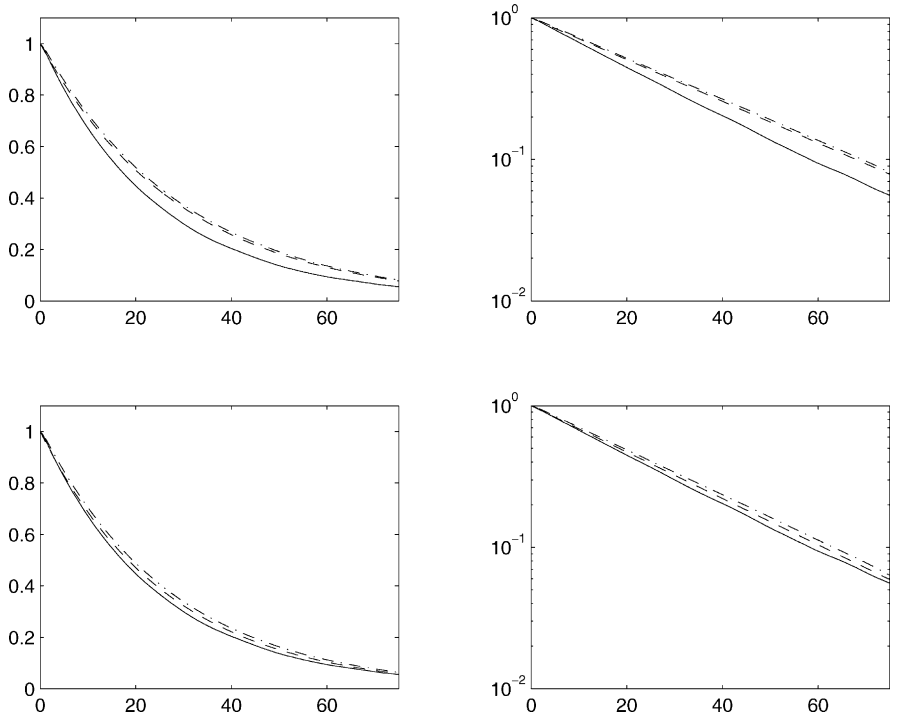

Fig. 17. Coupled truncated Burgers–Hopf system: additive case. Correlation function of x_1. Solid line: original system; dash-dotted line: stochastic model; dashed line: effective equations. The figures on top use $\gamma_k = \gamma_k^{\mathrm{dns}}$; and the bottom figures use $\gamma_k = \gamma_k^{\mathrm{adj}}$. The graphs with $\gamma_k = \gamma_k^{\mathrm{scal}}$ in are not shown since they are barely different than the one with $\gamma_k = \gamma_k^{\mathrm{dns}}$ (see (99)).

3.3. *Coupled truncated Burgers–Hopf system with two additional modes: multiplicative case*

The next extension of the truncated Burgers–Hopf system which we shall study is ($1 \le k, |p|, |q| \le \Lambda$)

$$\frac{\mathrm{d}x_1}{\mathrm{d}t} = \lambda \sum_k (b_k^{1|2y} x_2 y_k + b_k^{1|2z} x_2 z_k), \qquad \frac{\mathrm{d}x_2}{\mathrm{d}t} = \lambda \sum_k (b_k^{2|1y} x_1 y_k + b_k^{2|1z} x_2 z_k),$$
$$\frac{\mathrm{d}y_k}{\mathrm{d}t} = -\mathrm{Re}\,\frac{\mathrm{i}k}{2} \sum_{p+q+k=0} \hat{u}_p^* \hat{u}_q^* + \lambda b_k^{y|12} x_1 x_2, \qquad \frac{\mathrm{d}z_k}{\mathrm{d}t} = -\mathrm{Im}\,\frac{\mathrm{i}k}{2} \sum_{p+q+k=0} \hat{u}_p^* \hat{u}_q^* + \lambda b_k^{z|12} x_1 x_2, \tag{102}$$

where the interaction coefficients are of order 1 and satisfy

$$b_k^{1|2y} + b_k^{2|1y} + b_k^{y|12} = 0, \qquad b_k^{1|2z} + b_k^{2|1z} + b_k^{z|12} = 0. \tag{103}$$

Here modes (x_1, x_2) are driven by the Burgers–Hopf bath, (y_k, z_k), and we will derive a closed set of stochastic differential equations for (x_1, x_2) alone by suitable elimination of the bath using the theory from Majda et al. [5,6]. Note that the nonlinear terms containing any given triple, $(x_{1,2}, y_k, z_k)$, k fixed, in the right-hand side of the equations in (102) are of the same type as in the multiplicative triad model. Thus we can expect that the reduced equations for (x_1, x_2) alone obtained from (102) will contain nonlinear corrections in (x_1, x_2) as well as multiplicative noises. We confirm this below by studying the equations in (102) in the regime where

$$\beta = 50, \qquad \Lambda = 50, \qquad \lambda = 3 \tag{104}$$

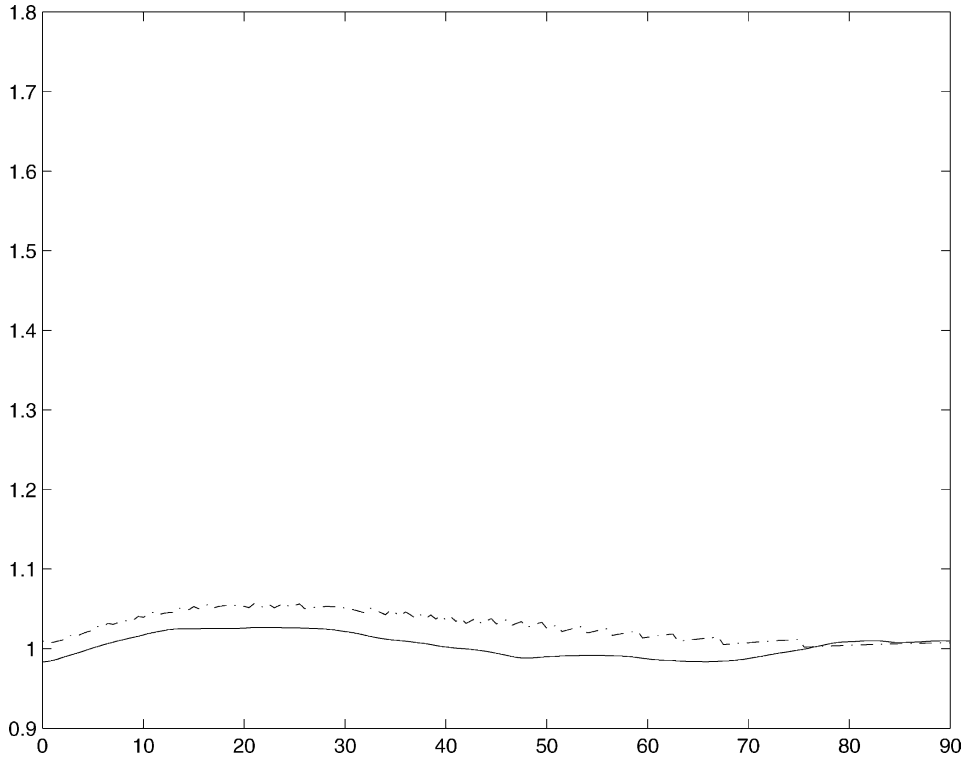

Fig. 18. Coupled truncated Burgers–Hopf system: additive case. The two-time fourth-order moment $K_1(t)$ defined in (101) and measuring the time-correlation of the energy $x_1^2(t)$ in mode $x_1(t)$. A Gaussian process implies no correlation in energy and $K_1(t) = 1$. This figure has the same vertical scale as, and should be compared to, Figs. 22 and 26.

(β is again related to the constant energy in the system, see (109)) and with the interaction coefficients $b_k^{\cdot|\cdot\cdot}$ as listed in Table 4. As in the additive case, these coefficients were generated randomly within $[-1, 1]$ under the constraint (103). The equations in (102) were integrated numerically as the equations in (72).

3.3.1. *Stationary distribution*

The system in (72) conserves the following energy because of the constraints in (103):

$$E = x_1^2 + x_2^2 + \sum_{k=1}^{\Lambda} |u_k|^2 = x_1^2 + x_2^2 + \sum_{k=1}^{\Lambda} (y_k^2 + z_k^2), \tag{105}$$

Table 4
Coupled truncated Burgers–Hopf system: multiplicative case. Interaction coefficients

k	$b_k^{y\|12}$	$b_k^{1\|2y}$	$b_k^{2\|1y}$	$b_k^{z\|12}$	$b_k^{1\|2z}$	$b_k^{2\|1z}$
1	0.2498	−0.5933	0.3435	0.4205	0.4979	−0.9183
2	0.3488	−0.8316	0.4829	0.2268	0.2461	−0.4729
3	0.3514	−0.6200	0.2687	0.3240	0.4440	−0.7680
4	0.3131	−0.5795	0.2664	0.3719	0.2741	−0.6459
5	0.4662	−0.7353	0.2690	0.4359	0.3450	−0.7809

and has the Liouville property,

$$0 = \frac{\partial F_{x_1}}{\partial x_1} + \frac{\partial F_{x_2}}{\partial x_2} + \sum_{k=1}^{\Lambda} \left(\frac{\partial F_{y_k}}{\partial y_k} + \frac{\partial F_{z_k}}{\partial z_k} \right), \tag{106}$$

where $F_{x_1}, \ldots$ denote the respective right-hand sides of the equations in (102). As a result the Gaussian Gibbs measure with density

$$p_\beta = Z^{-1} \exp(-\beta E) = Z^{-1} \exp\left(-\beta \left(x_1^2 + x_2^2 + \sum_{k=1}^{\Lambda} (y_k^2 + z_k^2) \right) \right), \tag{107}$$

is a stationary distribution for the dynamics in (102) and, as for (79) in the additive case, the numerical results support that (107) is in fact the appropriate stationary distribution for the system in (102) at fixed energy. The density in (106) implies equipartition of energy among modes (x_1, x_2) and the bath variables (y_k, z_k)

$$\operatorname{cov}(x_1) = \operatorname{cov}(x_2) = \operatorname{cov}(y_k) = \operatorname{cov}(z_k) = \frac{1}{2\beta}, \tag{108}$$

and the parameter β is uniquely determined by the energy in (105) computed on the initial condition, E_0

$$\frac{1}{2\beta} = \frac{E_0}{2 + 2\Lambda}. \tag{109}$$

As in [15,16], the numerical experiments confirm the predictions in (107) and (108). The first few moments of x_1, and x_2 consistent with these predictions are listed in Table 5.

3.3.2. *Stochastic modeling and stochastic consistency*

Following [5,6], we apply the same stochastic modeling assumption as in the additive case, i.e. we use (81) to represent the nonlinear self-interaction of the bath modes, (y_k, z_k), in (102). Thus we replace the original system in (102) by the stochastic model

$$\begin{aligned} \frac{\mathrm{d}x_1}{\mathrm{d}t} &= \lambda \sum_k (b_k^{1|2y} x_2 y_k + b_k^{1|2z} x_2 z_k), & \frac{\mathrm{d}x_2}{\mathrm{d}t} &= \lambda \sum_k (b_k^{2|1y} x_1 y_k + b_k^{2|1z} x_2 z_k), \\ \frac{\mathrm{d}y_k}{\mathrm{d}t} &= \lambda b_k^{y|12} x_1 x_2 - \gamma_k y_k + \sigma_k \dot{W}_k^y(t), & \frac{\mathrm{d}z_k}{\mathrm{d}t} &= \lambda b_k^{z|12} x_1 x_2 - \gamma_k z_k + \sigma_k \dot{W}_k^z(t). \end{aligned} \tag{110}$$

Depending on the number of $b^{1|2\cdot}$ and $b^{2|1\cdot}$ that are non-zero, the stochastic model in (110) may involve a smaller number of equations than the original system in (102). Recall that in our simulations, we took $\Lambda = 50$, but $b^{1|2\cdot}$, and $b^{2|1\cdot}$ non-zero for the first five modes only. The equations in (110) were integrated numerically using the same procedure as in the additive case.

Table 5
Coupled truncated Burgers–Hopf system: multiplicative case. One point statistics of x_1 and x_2

	Stat Mech	DNS
$\langle x_1 \rangle$	0	−0.0008
$\langle x_2 \rangle$	0	−0.0005
$\langle x_1^2 \rangle$	0.01	0.0099
$\langle x_2^2 \rangle$	0.01	0.0099
$\langle x_1^4 \rangle$	0.0003	0.000304
$\langle x_2^4 \rangle$	0.0003	0.000302

The parameters σ_k and γ_k are determined as in the additive case so as to achieve optimal stochastic consistency between (102) and (110). We take the ratio σ_k^2/γ_k equal to $1/\beta$ as in (83) in order that the stationary distribution for (102) has the density in (107). It remains to determine γ_k, say, and here we only consider procedure P2 based on taking the $\gamma_k = \gamma_k^{\mathrm{dns}}$ where γ_k^{dns} is the normalized area below the actual correlation functions obtained by direct numerical simulations of the original system in (102). In fact, for the range of parameters we considered, in this example procedure P2 produces essentially the same values as procedure P3. Recall that for P3 one picks the γ_k^{adj} for which the correlation functions of the bath modes predicted by the stochastic model in (110) reproduce best the exponential functions

$$\frac{\mathrm{e}^{-\gamma_k^{\mathrm{dns}} t}}{2\beta}. \tag{111}$$

Also recall that in general $\gamma_k^{\mathrm{adj}} \neq \gamma_k^{\mathrm{dns}}$ (see the discussion in Section 3.2.2) but in the present case the difference was not noticeable, i.e. $\gamma_k^{\mathrm{adj}} \approx \gamma_k^{\mathrm{dns}}$. This can be seen in Fig. 19. The corresponding values of γ_k^{dns} are listed in Table 6.

The value of ε can be estimated similarly as in the additive case using the two procedures explained in Section 3.2.3. The empirical $\varepsilon^{\mathrm{emp}}$ obtained from the decay rates of the resolved modes (x_1, x_2) and the modes from the bath

$$\varepsilon^{\mathrm{emp}} = \sqrt{\frac{\text{slowest time-scale of the unresolved modes, } (y_k, z_k)}{\text{fastest time-scale of the resolved modes, } (x_1, x_2)}}, \tag{112}$$

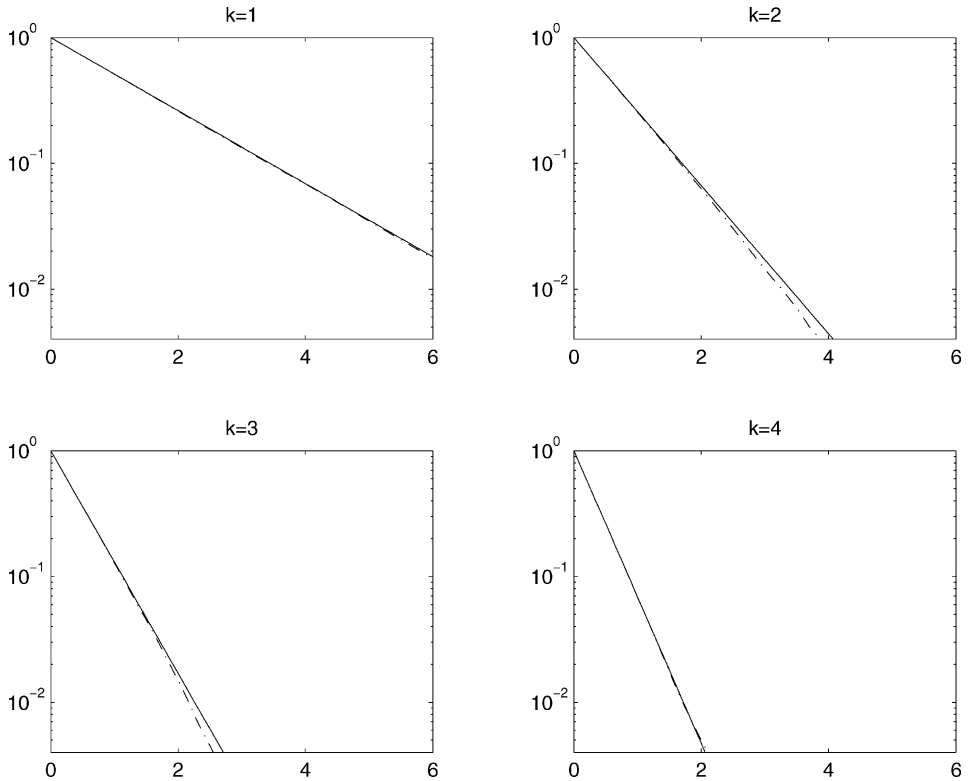

Fig. 19. Coupled truncated Burgers–Hopf system: multiplicative case. Comparison of correlation functions of $y_k = \mathrm{Re}\, u_k, k = 1, \ldots, 4$ predicted by the stochastic model (solid line) and the functions $\mathrm{e}^{-\gamma_k^{\mathrm{dns}} t}/2\beta$ (dashed line).

Table 6
Coupled truncated Burgers–Hopf system: multiplicative case. Estimates for the decay rates of the correlation functions of the bath

k	γ_k^{dns}
1	0.668
2	1.355
3	2.037
4	2.678
5	3.319

gives using the data from numerical simulations

$$\varepsilon^{\mathrm{emp}} = 0.53.$$

On the other hand, the a priori ε,

$$\varepsilon = \frac{\lambda}{\gamma_{k=1}\sqrt{2\beta}}, \tag{113}$$

gives

$$\varepsilon = 0.41.$$

Both values agree fairly well in this example, and, considering how big they are, mode elimination works surprisingly well as we show next.

3.3.3. *Mode elimination*

The following closed system of equations for (x_1, x_2) is obtained from the stochastic model in (82) by elimination of the unresolved variables, (y_k, z_k) [6]:

$$\begin{aligned}
\frac{\mathrm{d}x_1}{\mathrm{d}t} &= -\lambda^2\bar{\gamma}x_1 - \lambda^2 N_1 x_2^2 x_1 + \lambda\bar{\sigma}_{11}x_2\dot{W}_1(t) + \lambda\bar{\sigma}_{12}x_2\dot{W}_2(t),\\
\frac{\mathrm{d}x_2}{\mathrm{d}t} &= -\lambda^2\bar{\gamma}x_2 - \lambda^2 N_2 x_1^2 x_2 + \lambda\bar{\sigma}_{21}x_1\dot{W}_1(t) + \lambda\bar{\sigma}_{22}x_1\dot{W}_2(t).
\end{aligned} \tag{114}$$

As for the multiplicative triad system, these equations can be obtained by solving the equations for (y_k, z_k) in (110) at given (x_1, x_2), substituting these solutions in the equations for (x_1, x_2), and performing asymptotic expansion in ε. Here $W_1(t)$ and $W_2(t)$ are independent Wiener processes and the various parameters are defined as follows. Let

$$\begin{aligned}
A &= \beta^{-1}\sum_{k=1}^{\Lambda}\gamma_k^{-1}((b_k^{1|2y})^2 + (b_k^{1|2z})^2), \qquad B = \beta^{-1}\sum_{k=1}^{\Lambda}\gamma_k^{-1}((b_k^{2|1y})^2 + (b_k^{2|1z})^2),\\
C &= \beta^{-1}\sum_{k=1}^{\Lambda}\gamma_k^{-1}(b_k^{1|2y}b_k^{2|1y} + b_k^{1|2z}b_k^{2|1z}).
\end{aligned} \tag{115}$$

Then

$$\bar{\gamma} = -\tfrac{1}{2}C, \qquad N_1 = \beta(A + C), \qquad N_2 = \beta(B + C), \tag{116}$$

and the matrix $\bar{\sigma}$, which is defined as

$$\bar{\sigma} = \begin{pmatrix} \bar{\sigma}_{11} & \bar{\sigma}_{12} \\ \bar{\sigma}_{21} & \bar{\sigma}_{22} \end{pmatrix}, \tag{117}$$

is such that

$$\bar{\sigma}\bar{\sigma}^{\mathrm{T}} = \begin{pmatrix} A & C \\ C & B \end{pmatrix}. \tag{118}$$

Using Cauchy–Schwartz, it is easy to see that the matrix in (118) is positive definite, hence its square-root $\bar{\sigma}$ exists. Of course $\bar{\sigma}$ is not unique, and it is always possible to make it symmetric, $\bar{\sigma} = \bar{\sigma}^{\mathrm{T}}$, i.e. $\bar{\sigma}_{12} = \bar{\sigma}_{21}$.

Though the solution of the equations in (114) is not available, the stationary distribution for the process (x_1, x_2) has a density given precisely by the Gaussian in (107) (projected on modes (x_1, x_2)). This can be seen [6] upon noting that (107) is annihilated by the adjoint of the Fokker–Planck operator associated with (114)

$$L = -\lambda^2(\bar{\gamma}x_1 + N_1x_2^2x_1)\frac{\partial}{\partial x_1} - \lambda^2(\bar{\gamma}x_2 + N_2x_1^2x_2)\frac{\partial}{\partial x_2} + \lambda^2 Ax_2^2\frac{\partial^2}{\partial x_1^2} + \lambda^2 Bx_1^2\frac{\partial^2}{\partial x_2^2} + 2\lambda^2 Cx_1x_2\frac{\partial^2}{\partial x_1\partial x_2}. \tag{119}$$

To further check the relevance of the reduced stochastic model in (114) for the original dynamics in (102), we compute averaged quantities involving two times. The reduced equations in (114) were integrated by time-splitting, using a second-order Runge–Kutta algorithm for the nonlinear terms, and the strong Milstein scheme of order 1 for the stochastic terms [20]. The parameters used in the simulations give the following values for A, B, and C:

$$A = 0.3762, \qquad B = 0.4478, \qquad C = -0.3392.$$

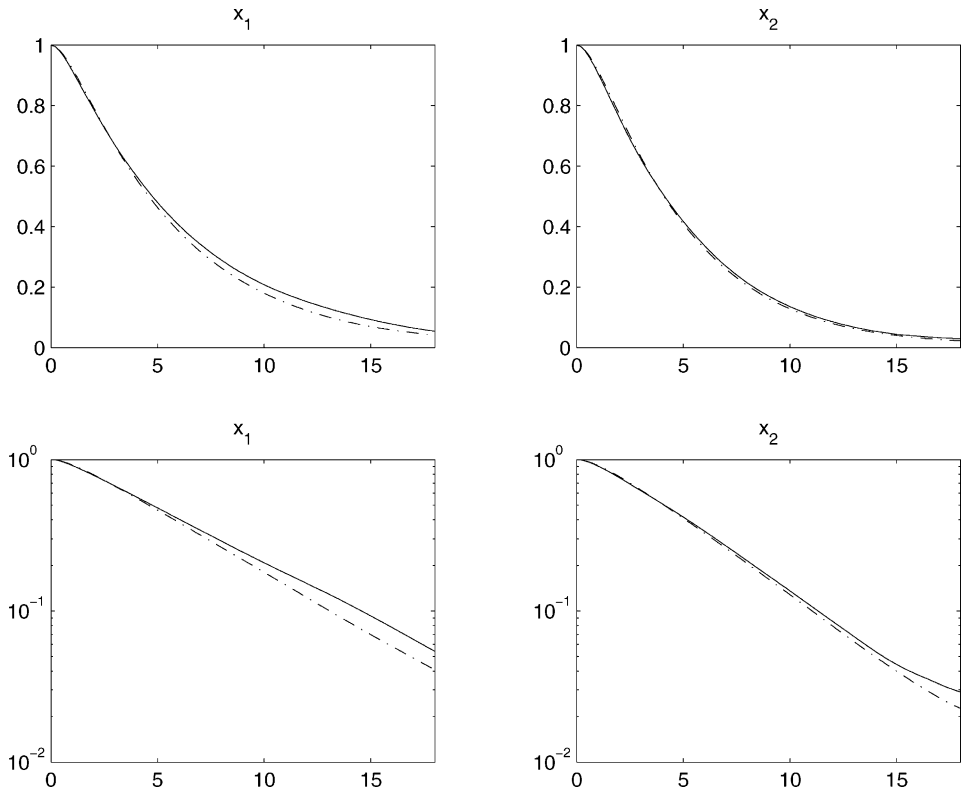

Fig. 20. Coupled truncated Burgers–Hopf system: multiplicative case. Comparison of the time-correlation functions of x_1 and x_2 predicted by the original system (solid line) and the stochastic model (dash-dotted line).

This gives

$$\bar{\gamma} = 0.17, \qquad N_1 = 1.85, \qquad N_2 = 5.43, \tag{120}$$

and we selected $\bar{\sigma}$ consistent with (117) as

$$\bar{\sigma}_{11} = 0.241, \qquad \bar{\sigma}_{12} = -0.564, \qquad \bar{\sigma}_{22} = 0.360. \tag{121}$$

We computed first the time-correlation functions

$$C_1(t) = \langle x_1(t+s)x_1(s)\rangle, \qquad C_2(t) = \langle x_2(t+s)x_2(s)\rangle.$$

It can be seen in Fig. 20 that the agreement between the predictions of the original system in (102) and the stochastic model in (110) is excellent. The agreement between the predictions of the original system in (102) and the reduced equations in (114) is also very good, as can be seen in Fig. 21. The reduced equations (but not the stochastic model) actually miss the fact that the time-correlation functions are smooth at time $t = 0$. This is understandable and is a general feature of first-order Markov models, since those short time effects happen in fact on a (dimensionless) time-scale of order ε which is not captured by the reduced equations. On the other hand, these equations (as the stochastic model) actually reproduce very well the long-time decay of these functions. After the short transient, the correlation functions are in fact very close to exponentials with decay rates given in Table 7.

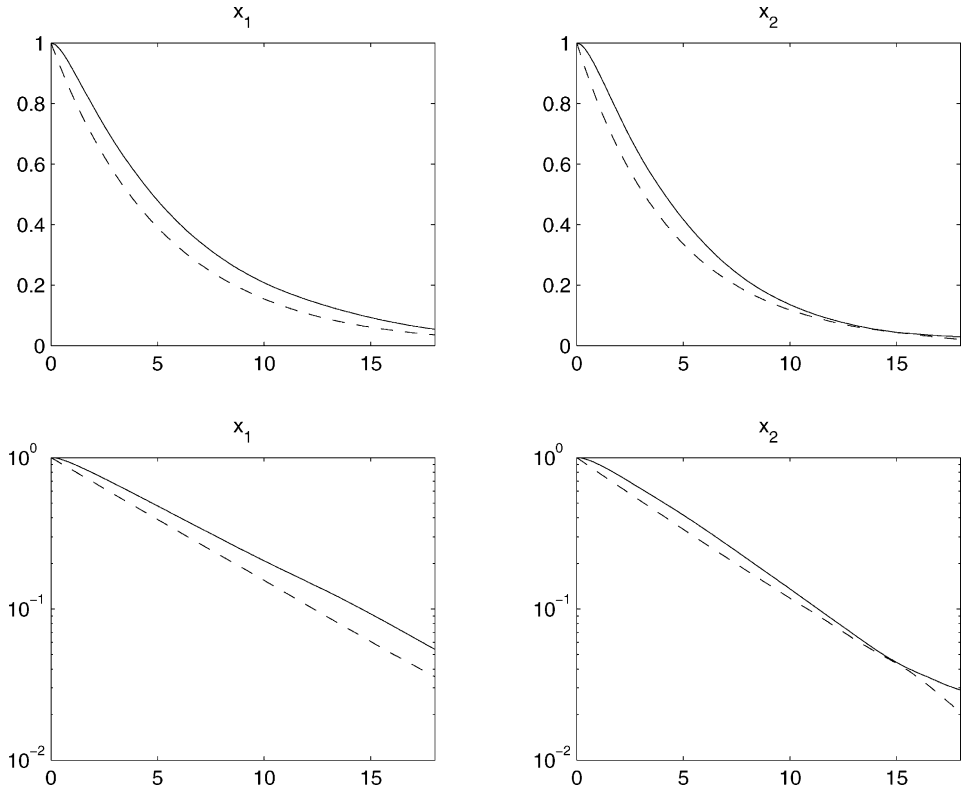

Fig. 21. Coupled truncated Burgers–Hopf system: multiplicative case. Comparison of the time-correlation functions of x_1 and x_2 predicted by the original system (solid line) and the reduced equations (dashed line).

Table 7
Coupled truncated Burgers–Hopf system: multiplicative case. Long-time decay rates for modes (x_1, x_2)

	Original system	Stochastic model	Reduced equations
γ_{x_1}	0.165	0.171	0.183
γ_{x_2}	0.179	0.182	0.215

We also computed the following quantities involving two-time fourth-order moments displayed in Fig. 22:

$$K_j(t) = \frac{\langle x_j^2(t+s)x_j^2(s)\rangle}{\langle x_j^2\rangle^2 + 2\langle x_j(t+s)x_j(s)\rangle^2}, \quad j = 1, 2. \tag{122}$$

These quantities actually measure the time-correlation of the energy $x_j^2(t)$ in mode $j = 1, 2$. For Gaussian processes, $K_j = 1$ for all times, implying in fact that there is no correlation between the energy computed at successive time. In contrast, in the present example, there is a significant departure from Gaussianity, in the order of 50%, for the original system in (102) and this departure is reproduced very well by both the stochastic model in (110) and the reduced equations in (114). It should be stressed that such departure *cannot* be obtained from linear Langevin models of Ornstein–Uhlenbeck type usually adopted in standard modeling procedures, and we must conclude that the multiplicative nature of the reduced equations in (114) is essential.

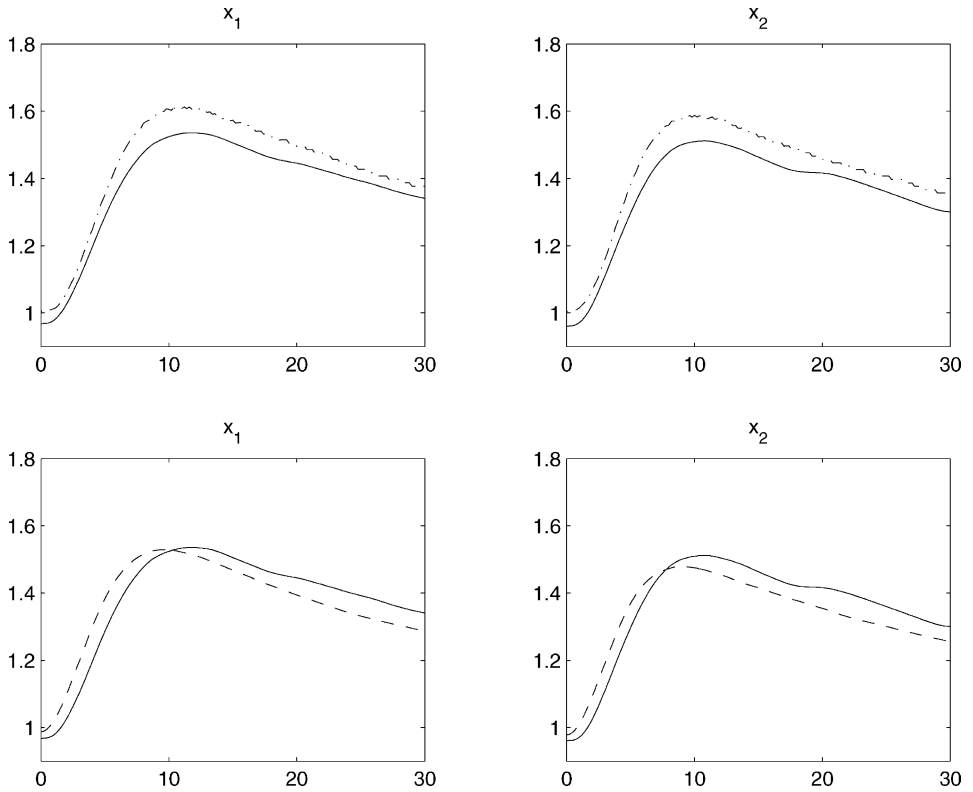

Fig. 22. Coupled truncated Burgers–Hopf system: multiplicative case. The two-time fourth-order moments $K_j(t)$, $j = 1, 2$ defined in (122) and measuring the time-correlation of the energy $x_j^2(t)$, $j = 1, 2$. The departure from Gaussianity observed in the original system (solid line) are well reproduced by both the stochastic model (dot-dashed line, top figures) and the reduced equations (dashed line, bottom figures).

3.4. Coupled truncated Burgers–Hopf system with two additional modes: combined case

The last extension of the truncated Burgers–Hopf system which we shall consider here is the following ($1 \le k, |p|, |q| \le \Lambda$):

$$\begin{aligned}
\frac{\mathrm{d}x_1}{\mathrm{d}t} &= \lambda_\mathrm{a} \sum_k b_k^{1|yz} y_k z_k + \lambda_\mathrm{m} \sum_k (b_k^{1|2y} x_2 y_k + b_k^{1|2z} x_2 z_k),\\
\frac{\mathrm{d}x_2}{\mathrm{d}t} &= \lambda_\mathrm{a} \sum_k b_k^{2|yz} y_k z_k + \lambda_\mathrm{m} \sum_k (b_k^{2|1y} x_1 y_k + b_k^{2|1z} x_2 z_k),\\
\frac{\mathrm{d}y_k}{\mathrm{d}t} &= -\mathrm{Re}\,\frac{\mathrm{i}k}{2} \sum_{p+q+k=0} \hat{u}_p^* \hat{u}_q^* + \lambda_\mathrm{a} b_k^{y|1z} x_1 z_k + \lambda_\mathrm{a} b_k^{y|2z} x_2 z_k + \lambda_\mathrm{m} b_k^{y|12} x_1 x_2,\\
\frac{\mathrm{d}z_k}{\mathrm{d}t} &= -\mathrm{Im}\,\frac{\mathrm{i}k}{2} \sum_{p+q+k=0} \hat{u}_p^* \hat{u}_q^* + \lambda_\mathrm{a} b_k^{z|1y} x_1 y_k + \lambda_\mathrm{a} b_k^{z|2y} x_2 y_k + \lambda_\mathrm{m} b_k^{z|12} x_1 x_2,
\end{aligned} \tag{123}$$

where $u_k = y_k + \mathrm{i}z_k$. This system is a combination of the additive model considered in Section 3.2 (with two resolved modes instead of one) and the multiplicative model considered in Section 3.3. The parameter λ_a is in front of the terms involved in coupling of additive type, while the parameter λ_m is in front of the terms involved in coupling of multiplicative type. The coupling coefficients $b_k^{\cdot|\cdot\cdot}$ are all of order 1 and satisfy (compare (73) and (103))

$$\begin{aligned}
&b_k^{1|yz} + b_k^{y|1z} + b_k^{z|1y} = 0, \qquad b_k^{2|yz} + b_k^{y|2z} + b_k^{z|2y} = 0,\\
&b_k^{1|2y} + b_k^{2|1y} + b_k^{y|12} = 0, \qquad b_k^{1|2z} + b_k^{2|1z} + b_k^{z|12} = 0.
\end{aligned} \tag{124}$$

Since the system in (123) combines additive and multiplicative features we expect that the reduced equations for modes (x_1, x_2) provided by mode elimination will involve both linear Langevin terms of Ornstein–Uhlenbeck type and nonlinear correction with multiplicative noise. This is indeed what we obtain below.

We shall study the system in (123) in the parameter regime

$$\beta = 50, \qquad \Lambda = 50, \qquad \lambda_\mathrm{a} = 4, \qquad \lambda_\mathrm{m} = 3 \tag{125}$$

(β is related to the constant energy in the system, see (109)) and with the interaction coefficients $b_k^{\cdot|\cdot\cdot}$ as listed in Tables 4 (multiplicative interaction terms) and 8 (additive interaction terms). The λ_m and the $b_k^{\cdot|\cdot\cdot}$'s involved in the multiplicative interaction terms are in fact exactly the same as the ones we took in Section 3.3. The equations in (123) were integrated numerically using the same scheme as in Section 3.3.

The system in (123) conserves the energy in (105) and has the Liouville property in (106) due to the constraints in (124). As a result, the measure with the Gaussian density in (107) is a stationary distribution for the dynamics in

Table 8
Coupled truncated Burgers–Hopf system: combined case. Interaction coefficients for the additive interaction terms

k	$b_k^{1\|yz}$	$b_k^{y\|1z}$	$b_k^{z\|1y}$	$b_k^{2\|yz}$	$b_k^{y\|2z}$	$b_k^{z\|2y}$
1	−0.4094	0.2894	0.1200	−0.3862	0.3325	0.0537
2	−0.3906	0.3438	0.0469	0.4963	0.4253	−0.9216
3	−0.6562	0.1500	0.5062	−0.5344	0.4219	0.1125
4	−0.4125	0.7303	−0.3178	0.6200	−0.2525	−0.3675
5	0.5275	0.4603	−0.9878	0.5925	0.1953	−0.7878

Table 9
Coupled truncated Burgers–Hopf system: combined case. One point statistics for the modes (x_1, x_2)

	Stat Mech	DNS
$\langle x_1 \rangle$	0	−0.001
$\langle x_2 \rangle$	0	−0.00007
$\langle x_1^2 \rangle$	0.01	0.00966
$\langle x_2^2 \rangle$	0.01	0.00965
$\langle x_1^4 \rangle$	0.0003	0.0003008
$\langle x_1^4 \rangle$	0.0003	0.0002977

(123), and the numerical results confirm that it is the appropriate (at fixed energy, see (109)) stationary distribution for this dynamics. Thus, at equilibrium we have again equipartition of energy as in (108). This is confirmed in Table 9 where we list the first few moments of (x_1, x_2) obtained from numerics.

3.4.1. *Stochastic modeling and stochastic consistency*

The stochastic modeling assumption is the same as in the additive and multiplicative cases. Thus we use (81) to represent the nonlinear self-interaction of the bath modes, (y_k, z_k), in the original system in (123) and we replace

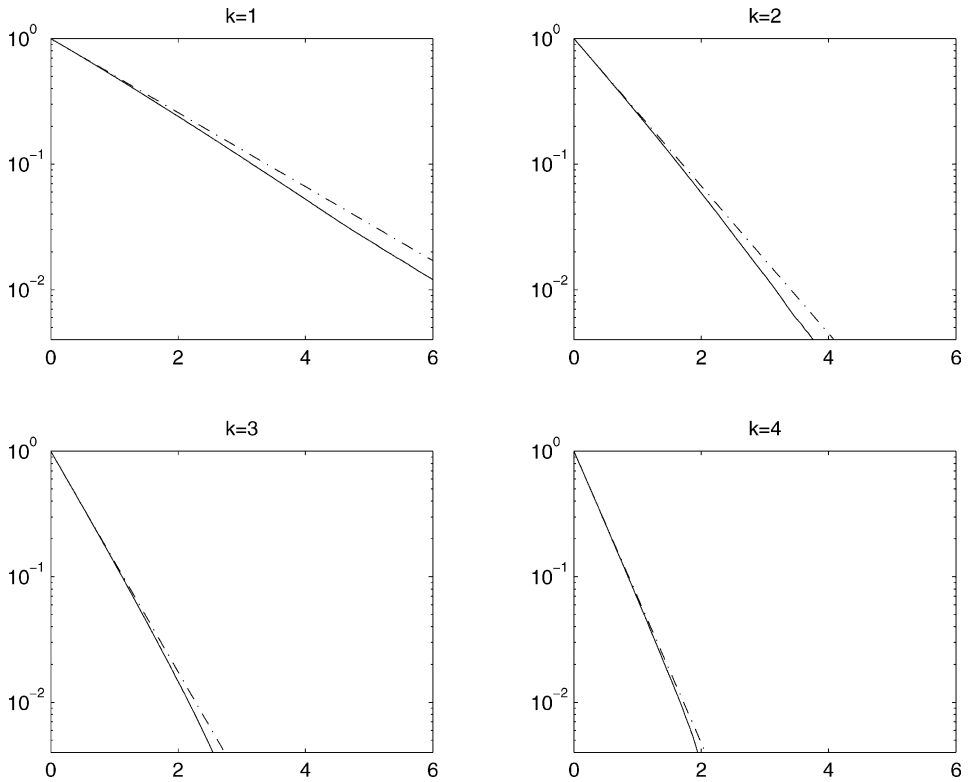

Fig. 23. Coupled truncated Burgers–Hopf system: combined case. Comparison of the correlation functions of the bath predicted by the stochastic model in (126) with $\gamma_k = \gamma_k^{\mathrm{dns}}$ (full lines) and the functions $\mathrm{e}^{-\gamma_k t}$ (dashed lines).

Table 10
Coupled truncated Burgers–Hopf system: combined case. Estimates for the decay rates of the correlation functions of the bath

k	γ_k^{dns}
1	0.6786
2	1.3513
3	2.0219
4	2.6740
5	3.2512

this system by

$$\begin{aligned}
\frac{\mathrm{d}x_1}{\mathrm{d}t} &= \lambda_{\mathrm{a}} \sum_k b_k^{1|yz} y_k z_k + \lambda_{\mathrm{m}} \sum_k (b_k^{1|2y} x_2 y_k + b_k^{1|2z} x_2 z_k),\\
\frac{\mathrm{d}x_2}{\mathrm{d}t} &= \lambda_{\mathrm{a}} \sum_k b_k^{2|yz} y_k z_k + \lambda_{\mathrm{m}} \sum_k (b_k^{2|1y} x_1 y_k + b_k^{2|1z} x_2 z_k),\\
\frac{\mathrm{d}y_k}{\mathrm{d}t} &= \lambda_{\mathrm{a}} b_k^{y|1z} x_1 z_k + \lambda_{\mathrm{a}} b_k^{y|2z} x_2 z_k + \lambda_{\mathrm{m}} b_k^{y|12} x_1 x_2 - \gamma_k y_k + \sigma_k \dot{W}_k^y(t),\\
\frac{\mathrm{d}z_k}{\mathrm{d}t} &= \lambda_{\mathrm{a}} b_k^{z|1y} x_1 y_k + \lambda_{\mathrm{a}} b_k^{z|2y} x_2 y_k + \lambda_{\mathrm{m}} b_k^{z|12} x_1 x_2 - \gamma_k z_k + \sigma_k \dot{W}_k^z(t).
\end{aligned} \tag{126}$$

In the parameter regime we consider, the stochastic model in (126) involves a smaller number of equations than the original system in (123) since we took $\Lambda = 50$, but the $b_k^{|\cdots}$'s are non-zero for the first five modes only. The equations in (126) were integrated numerically as the equations in (82) in the additive case.

The parameters σ_k and γ_k are again determined so as to achieve optimal stochastic consistency between (123) and (126). The ratio σ_k^2/γ_k is taken to be equal to $1/\beta$ as in (83) in order that the stationary distribution for (102) has the density in (107). We determine γ_k through procedure P2 based on taking the $\gamma_k = \gamma_k^{\mathrm{dns}}$ where γ_k^{dns} is the normalized area below the actual correlation functions obtained by direct numerical simulations of the original system in (123). As in the multiplicative case, for the range of parameters we considered, procedure P2 is essentially equivalent to the more refined procedure P3. The time-correlation functions predicted either by the original system in (123) or the stochastic model in (126) are compared in Fig. 23. The corresponding γ_k^{dns}'s are listed in Table 10.

The value of ε can be estimated exactly as in the multiplicative case. The empirical $\varepsilon^{\mathrm{emp}}$ obtained from the decay rates of the resolved modes (x_1, x_2) and the modes from the bath (see (112)) gives using the data from numerical simulations

$$\varepsilon^{\mathrm{emp}} = 0.54.$$

On the other hand, the a priori ε defined as

$$\varepsilon = \frac{\max(\lambda_{\mathrm{a}}, \lambda_{\mathrm{m}})}{\gamma_{k=1}\sqrt{2\beta}}, \tag{127}$$

gives

$$\varepsilon = 0.49.$$

Mode elimination will again work surprisingly well despite this large value of ε.

3.4.2. Mode elimination

Mode elimination produces the following closed system of equations for the two resolved variables (x_1, x_2) from the stochastic model in (126) [6]:

$$\begin{aligned}\frac{\mathrm{d}x_1}{\mathrm{d}t} &= -\lambda_{\mathrm{m}}^2\bar{\gamma}x_1 - \lambda_{\mathrm{m}}^2 N_1 x_2^2 x_1 + \lambda_{\mathrm{m}}\bar{\sigma}_{11}x_2\dot{W}_1(t) + \lambda_{\mathrm{m}}\bar{\sigma}_{12}x_2\dot{W}_2(t)\\ &\quad - \lambda_{\mathrm{a}}^2\gamma_{11}x_1 - \lambda_{\mathrm{a}}^2\gamma_{12}x_2 + \lambda_{\mathrm{a}}\sigma_{11}\dot{W}_3(t) + \lambda_{\mathrm{a}}\sigma_{12}\dot{W}_4(t),\\ \frac{\mathrm{d}x_2}{\mathrm{d}t} &= -\lambda_{\mathrm{m}}^2\bar{\gamma}x_2 - \lambda_{\mathrm{m}}^2 N_2 x_1^2 x_2 + \lambda_{\mathrm{m}}\bar{\sigma}_{21}x_1\dot{W}_1(t) + \lambda_{\mathrm{m}}\bar{\sigma}_{22}x_1\dot{W}_2(t) - \lambda_{\mathrm{a}}^2\gamma_{12}x_1\\ &\quad - \lambda_{\mathrm{a}}^2\gamma_{22}x_2 + \lambda_{\mathrm{a}}\sigma_{12}\dot{W}_3(t) + \lambda_{\mathrm{a}}\sigma_{22}\dot{W}_4(t).\end{aligned} \tag{128}$$

The terms involving λ_{m} arise because of the interactions of multiplicative type in the stochastic model in (126). In fact, the coefficient $\bar{\gamma}$, N_1, N_2, and $\bar{\sigma}$ entering (126) are identical with the ones entering (114) (see (115)–(118)) and their numerical values in the parameter regime we consider are given by

$$\bar{\gamma} = 0.17, \qquad N_1 = 1.89, \qquad N_2 = 5.39, \qquad \bar{\sigma}_{11} = 0.241, \qquad \bar{\sigma}_{12} = \bar{\sigma}_{21} = -0.563, \qquad \bar{\sigma}_{22} = 0.358. \tag{129}$$

(Those values are slightly different from the ones in (120) and (121) because the γ_k^{dns} are slightly different.) The

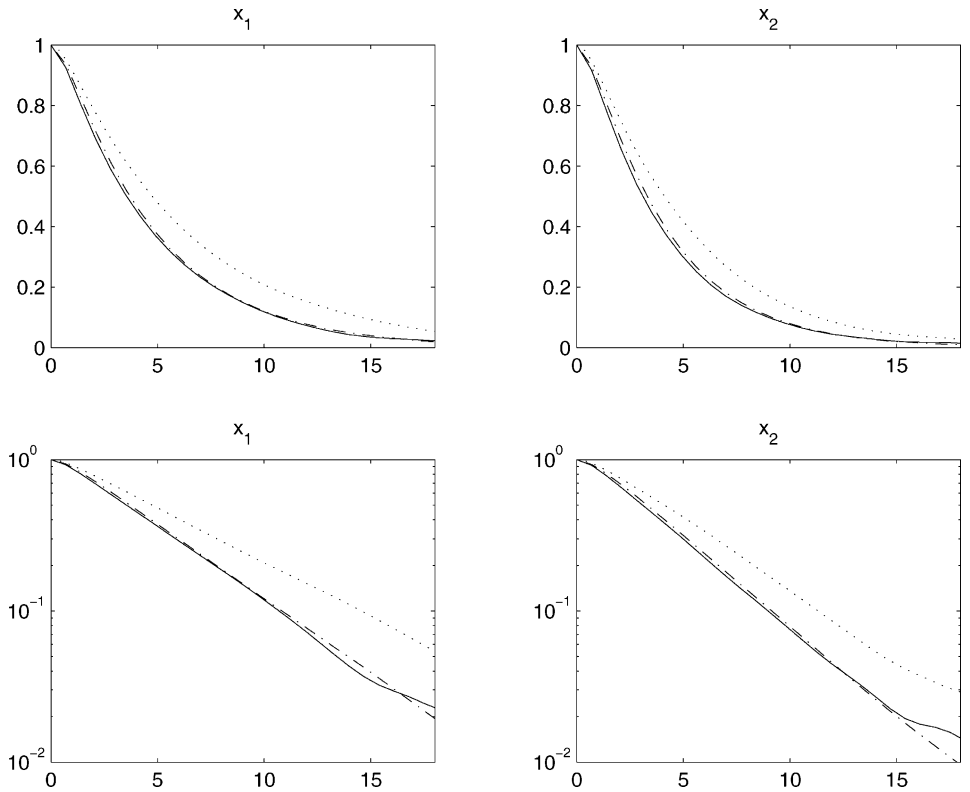

Fig. 24. Coupled truncated Burgers–Hopf system: combined case. Comparison of the time-correlation functions of x_1 and x_2 predicted by the original system (solid line) and the stochastic model (dash-dotted line). The dotted lines are the predictions from the coupled truncated Burgers–Hopf system in the multiplicative case alone from Fig. 20.

terms involving λ_a arise because of the interactions of additive type in the stochastic model in (126). They are of Ornstein–Uhlenbeck type, though non-diagonal, with

$$\gamma_{11} = \frac{\lambda_a^2}{4\beta} \sum_{k=1}^{\Lambda} \gamma_k^{-1} (b_k^{1|yz})^2, \qquad \gamma_{22} = \frac{\lambda_a^2}{4\beta} \sum_{k=1}^{\Lambda} \gamma_k^{-1} (b_k^{2|yz})^2, \qquad \gamma_{12} = \frac{\lambda_a^2}{4\beta} \sum_{k=1}^{\Lambda} \gamma_k^{-1} b_k^{1|yz} b_k^{2|yz}. \tag{130}$$

The matrix σ, defined as

$$\sigma = \begin{pmatrix} \sigma_{11} & \sigma_{12} \\ \sigma_{21} & \sigma_{22} \end{pmatrix}, \tag{131}$$

is such that

$$\sigma\sigma^{\mathrm{T}} = \beta^{-1} \begin{pmatrix} \gamma_{11} & \gamma_{12} \\ \gamma_{12} & \gamma_{22} \end{pmatrix}. \tag{132}$$

The matrix at the right-hand side of (132) is positive definite as it should be, as can be seen using Cauchy–Schwartz. The matrix σ is not uniquely defined by (132) and we can always make it symmetric, $\sigma = \sigma^{\mathrm{T}}$, i.e. $\sigma_{12} = \sigma_{21}$. For the parameter regime we consider, we obtain

$$\begin{aligned} &\gamma_{11} = 0.0370, \quad \gamma_{22} = 0.0407, \quad \gamma_{12} = 0.0135, \quad \sigma_{11} = 0.0267, \\ &\sigma_{22} = 0.0281, \quad \sigma_{12} = 0.0049. \end{aligned} \tag{133}$$

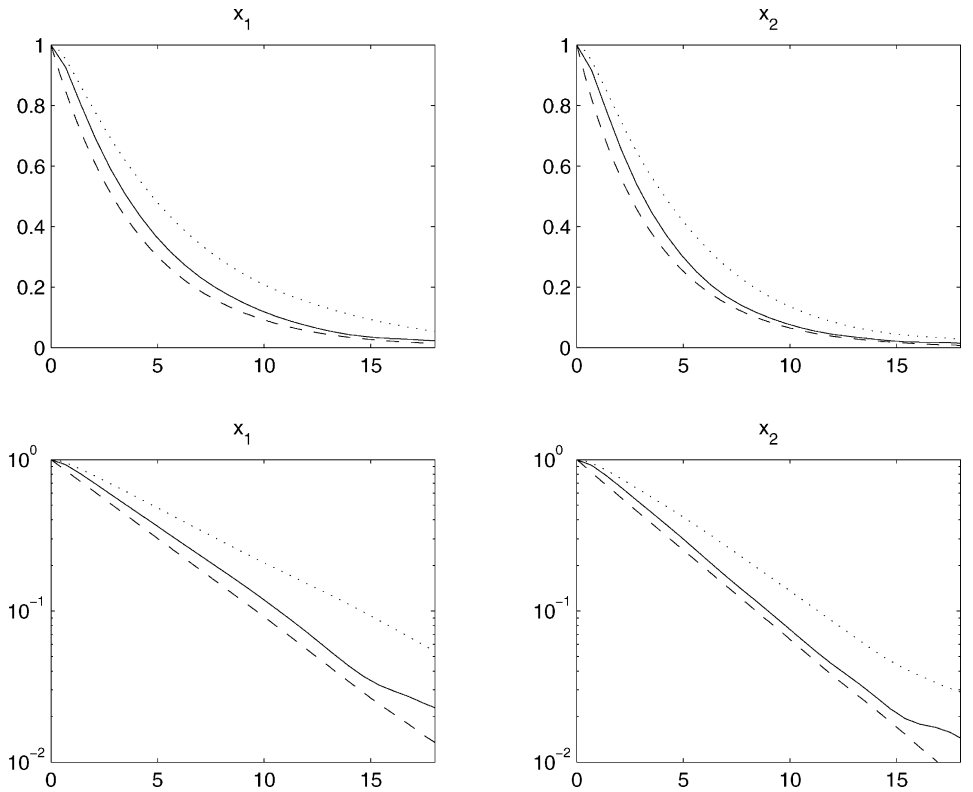

Fig. 25. Coupled truncated Burgers–Hopf system: combined case. Comparison of the time-correlation functions of x_1 and x_2 predicted by the original system (solid line) and the reduced equations (dashed line). The dotted lines are the predictions from the coupled truncated Burgers–Hopf system in the multiplicative case alone from Fig. 21.

Table 11
Coupled truncated Burgers–Hopf system: combined case. Long-time decay rates for modes (x_1, x_2)

	Original system	Stochastic model	Reduced equations
γ_{x_1}	0.178	0.185	0.233
γ_{x_2}	0.197	0.202	0.254

The solution of equations in (126) is not available but it can be checked that the stationary distribution for this process has the Gaussian density in (107). This can be seen upon noting that this density is annihilated by the adjoint of the Fokker–Planck operator associated with (128). The part of this operator associated with the multiplicative terms is (119) with λ_m substituted for λ; the part associated with the additive terms is

$$L' = -\lambda_a^2(\gamma_{11}x_1+\gamma_{12}x_2)\frac{\partial}{\partial x_1} - \lambda_a^2(\gamma_{12}x_1+\gamma_{22}x_2)\frac{\partial}{\partial x_2} + \lambda_a^2\gamma_{11}\frac{\partial^2}{\partial x_1^2} + \lambda_a^2\gamma_{22}\frac{\partial^2}{\partial x_2^2} + 2\lambda_a^2\gamma_{12}\frac{\partial^2}{\partial x_1\partial x_2}. \quad (134)$$

To check the relevance of the reduced equations in (128), we perform the same numerical tests involving two-time averages as the ones we used in the multiplicative case, and we utilize the same integration technique. The

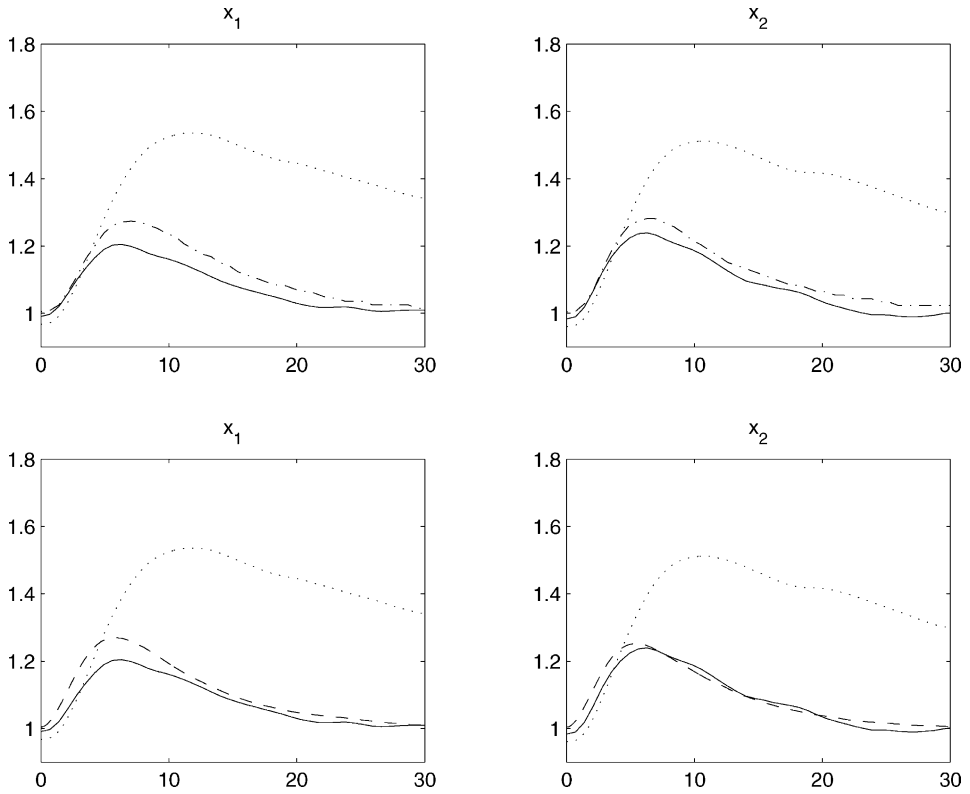

Fig. 26. Coupled truncated Burgers–Hopf system: combined case. The two-time fourth-order moments $K_j(t)$, $j = 1, 2$ defined in (122) and measuring the time-correlation of the energy $x_j^2(t)$, $j = 1, 2$. The departure from Gaussianity observed in the original system (solid line) are well reproduced by both the stochastic model (dot-dashed line, top figures) and the reduced equations (dashed line, bottom figures). The dotted lines are the predictions from the coupled truncated Burgers–Hopf system in the multiplicative case alone from Fig. 22.

time-correlation functions

$$C_1(t) = \langle x_1(t+s)x_1(s)\rangle, \qquad C_2(t) = \langle x_2(t+s)x_2(s)\rangle,$$

are shown in Figs. 24 and 25. For comparison, we also present the results for the multiplicative system of Section 3.3 where all the additive interactions are set to zero. The agreement between the predictions of the original system in (102) and both the stochastic model in (126) and the reduced equations in (128) is very good. As in the multiplicative case, the reduced equations (but not the stochastic model) miss the smooth start of the time-correlation functions but they actually reproduce very well the long-time decay of these functions. After the short transient, the correlation functions are very close to exponentials with decay rates given in Table 11. Notice that these rates indicate that the time-correlation functions decay faster in the combined than in the multiplicative case. This is due to the additional damping produced by the linear Langevin terms representing the additive interaction terms in the original system.

We also computed the two-time fourth-order moments given in (122) with the results presented in Fig. 26. Recall that these quantities actually measure the time-correlation of the energy $x_j^2(t)$ in mode $j = 1, 2$, and $K_j = 1$ for all times for a Gaussian process. In contrast, the original system in (123) produces significant departures from Gaussianity of over 25%, which are reproduced well both by the stochastic model in (126) and the reduced equations in (128). Here the multiplicative nature of the equations in (128) is again essential. Notice, however, that these departures are lower than in the multiplicative case, indicating that the linear Langevin terms actually deplete the non-Gaussian corrections in the process.

4. Concluding remarks

To recapitulate the highlights of this paper, we have shown that the stochastic modeling strategy proposed in [5,6] is applicable to non-trivial test cases which display features of vastly more complex systems. It was shown that a suitable stochastic modeling assumption on the original system gives a stochastic model which can achieve very good stochastic consistency with the original dynamics. Besides, the range of parameters where such stochastic consistency is observed can be determined a priori with consistent surprisingly large values of the coupling coefficients. We have also shown that the reduced equations for the essential degrees of freedom which are obtained by suitable projection of the stochastic model quantitatively capture non-trivial statistical features of the original dynamics, like the stationary distribution, or two-time statistical averages involving second and fourth moments. The structure of the reduced equations is unusual since, besides linear Langevin terms of Orstein–Ulhenbeck type, these equations may also involve nonlinear corrections in the essential modes and multiplicative noises. Yet, these features proved to be crucial for an adequate description of the original dynamics by the reduced equations as confirmed by the quantitative tests developed in this paper. As demonstrated here the reduced stochastic models are quantitatively capable of approximating the original problem with many degrees of freedom with surprisingly large values for the small parameter. We certainly hope that the techniques described here will be useful for stochastic modeling in many problems of scientific and engineering interest.

Acknowledgements

The research of A. Majda is partially supported by NSF grant DMS-9972865, ONR grant N00014-96-1-0043, and ARO grant DAAD19-01-10810. I. Timofeyev is supported as a postdoctoral fellow by NSF grant DMS-9972865 and ARO grant DAAD19-01-10810. E. Vanden-Eijnden is partially supported by NSF grant DMS-9510356.

References

[1] J. Pedlosky, Geophysical Fluid Dynamics, 2nd Edition, Springer, New York, 1987.
[2] D. Frenkel, B. Smit, Understanding Molecular Simulations. From Algorithms to Applications, Academic Press, San Diego, CA, 1996.
[3] A. Pimpinelli, J. Villain, Physics of Crystal Growth, Cambridge University Press, Cambridge, 1998.
[4] W.E. Selected problems in material science, in: B. Engquist, W. Schmid (Eds.), Mathematics Unlimited—2001 and Beyond, Springer, Berlin, 2001.
[5] A. Majda, I. Timofeyev, E. Vanden-Eijnden, Models for stochastic climate prediction, Proc. Natl. Acad. Sci. 96 (1999) 14687–14691.
[6] A. Majda, I. Timofeyev, E. Vanden-Eijnden, A mathematics framework for stochastic climate models, Commun. Pure Appl. Math. 54 (2001) 891–974.
[7] S. Griffies, E. Tziperman, A linear thermohaline oscillator driven by stochastic atmospheric forcing, J. Clim. 8 (1995) 2440–2453.
[8] J.A. Whitaker, P.D. Sardesmukh, A linear theory of extratropical synoptic eddy statistics, J. Atmos. Sci. 55 (1998) 237–258.
[9] U. Achatz, G. Branstator, A two-layer model with empirical linear corrections and reduced order for studies of internal climate variability, J. Atmos. Sci. 56 (1999) 3140–3160.
[10] Ch. Schütte, A. Fisher, W. Huisinga, P. Deuflhard, A direct approach to conformational dynamics based on hybrid Monte Carlo, J. Comp. Phys. 151 (1999) 146–168.
[11] T.G. Kurtz, A limit theorem for perturbed operator semigroups with applications to random evolutions, J. Funct. Anal. 12 (1973) 55–67.
[12] T.G. Kurtz, Semigroups of conditioned shifts and approximations of Markov processes, Ann. Probab. 3 (1975) 618–642.
[13] R.S. Ellis, M.A. Pinsky, The first and second fluid approximations to the linearized Boltzmann equation, J. Math. Pure Appl. 54 (9) (1975) 125–156.
[14] G. Papanicolaou, Some probabilistic problems and methods in singular perturbations, Rocky Mountain J. Math. 6 (1976) 653–673.
[15] A. Majda, I. Timofeyev, Remarkable statistical behavior for truncated Burgers–Hopf dynamics, Proc. Natl. Acad. Sci. 97 (2000) 12413–12417.
[16] A. Majda, I. Timofeyev, Statistical mechanics for truncations of the Burgers–Hopf equation: a model for intrinsic stochastic behavior with scaling, Milan J. Math. (former Rend. Sem. Math. Fis. Milano) 70 (1) (2002) 39–96.
[17] L. Arnold, Stochastic Differential Equations: Theory and Applications, Wiley, New York, 1974.
[18] R. Abramov, G. Kovacic, A.J. Majda, Hamiltonian structure and statistically relevant conserved quantities for the truncated Burgers–Hopf equation, Commun. Pure Appl. Math., accepted for publication.
[19] A. Majda, I. Timofeyev, E. Vanden-Eijnden, J. Atmos. Sci., submitted.
[20] P.E. Kloeden, E. Platen, Numerical Solutions of Stochastic Differential Equations, Springer, New York, 1995.